Boundary Value Problems
a SpringerOpen Journal

RESEARCH Open Access

Influence of moving heat sources on thermoviscoelastic behavior of rotating nanorods: a nonlocal Klein–Gordon perspective with fractional heat conduction

Ahmed E. Abouelregal[1*], M. Marin[2,3*], Abdelaziz Foul[4] and Sameh S. Askar[4]

*Correspondence:
ahabogal@mans.edu.eg;
m.marin@unitbv.ro
[1]Department of Mathematics, Faculty of Science, Mansoura University, Mansoura 35516, Egypt
[2]Department of Mathematics and Computer Science, Transilvania University of Brasov, Brasov, Romania
Full list of author information is available at the end of the article

Abstract

This study investigated magneto-thermoelastic interactions in rotating viscoelastic nanorods under moving heat sources, advancing the modeling of nanoscale systems. A key innovation was the adoption of Klein–Gordon-type nonlocal elasticity theory, which incorporated internal length and time scales to capture small-scale interactions effectively. Additionally, a fractional heat conduction model using two-parameter tempered-Caputo derivatives introduced memory effects and nonlocality, ensuring finite thermal wave speeds and overcoming the limitations of the classical Fourier model. The inclusion of the Kelvin–Voigt viscoelastic framework accounted for energy dissipation, enhancing the model's accuracy. By integrating rotation, viscoelasticity, magnetic forces, and fractional heat conduction, the study developed a comprehensive nonlinear model of nanorod behavior. Numerical simulations demonstrated that fractional-order heat conduction and nonlocal elasticity significantly influenced the thermal and mechanical responses, reducing discrepancies in heat propagation predictions. These findings showed that the fractional and tempering parameters controlled thermal dissipation rates and thermal wave propagation velocity, ensuring physically realistic thermal responses. The incorporation of nonlocal length scale and time scale parameters enabled accurate representation of size-dependent behaviors, including stiffness reduction and stress redistribution in nanorods. These parameters also influenced memory effects affecting wave propagation and relaxation in viscoelastic materials.

Keywords: Tempered-Caputo derivatives; Thermo-viscoelastic; Klein–Gordon type; Internal length and time scale; Nanorods

1 Introduction

Viscoelastic materials demonstrate a unique interplay of elastic and viscous behaviors when subjected to deformation, resulting in a response that is inherently time dependent. These materials possess characteristics of both solids and fluids; they can store energy similarly to elastic solids while also dissipating energy like viscous fluids. The viscoelastic response is significantly influenced by various factors, including time, temperature, fre-

quency, and the rate of loading, which collectively determine how these materials behave under different conditions [1].

Viscoelastic materials exhibit several distinct characteristics that define their behavior under stress and strain. One primary feature is their time-dependent behavior: the response of these materials depends on the duration of applied stress or strain. Unlike purely elastic materials, viscoelastic materials need time to return to their original shape after load removal. Stress relaxation is another important characteristic [2]. When under constant strain, the stress within the material gradually decreases over time as the material relaxes, demonstrating its ability to adapt to sustained deformations. Creep behavior manifests when these materials are subjected to constant stress. They progressively deform over time, further illustrating their time-dependent response to applied loads. Energy dissipation represents another key aspect of viscoelastic materials. During cyclic loading, they display a hysteresis loop, indicating that some input energy dissipates as heat rather than being fully recovered. This energy loss becomes critical in applications involving repeated loading. Temperature and loading frequency significantly influence viscoelastic response [2, 3]. At elevated temperatures or low frequencies, these materials behave more like viscous fluids. Conversely, at lower temperatures or higher frequencies, they exhibit characteristics closer to elastic solids. This temperature and frequency dependence proves crucial for predicting viscoelastic material performance across various applications [4].

To mathematically characterize viscoelastic behavior, various mechanical models are employed, often combining springs (representing elastic elements) and dashpots (representing viscous elements). The Maxwell model consists of a spring and dashpot arranged in series. This model effectively describes stress relaxation, capturing how stress decreases over time under constant strain [5]. However, it inadequately represents creep behavior, failing to account for progressive deformation under constant stress. The Kelvin–Voigt model features a spring and dashpot arranged in parallel [6]. While this configuration effectively captures creep behavior under constant stress, it fails to adequately describe stress relaxation phenomena [7].

In recent decades, fractional calculus has gained recognition as a robust mathematical framework for modeling and analyzing a diverse array of physical phenomena, especially those characterized by complex, anomalous, or memory-dependent behaviors [8]. Classical calculus focuses on integer-order derivatives and integrals; in contrast, fractional calculus extends these concepts to noninteger (fractional) orders. This generalization enables a more precise representation of processes that exhibit long-term memory, nonlocality, and hereditary effects, making it particularly valuable in fields such as physics, engineering, and applied mathematics [9].

Fractional calculus has emerged as a powerful mathematical tool across diverse scientific fields, offering enhanced modeling capabilities for complex physical phenomena. In thermal sciences and transport phenomena, fractional calculus addresses limitations of classical approaches. It models anomalous heat conduction and diffusion processes where the laws of Fourier and Fick prove inadequate, particularly in heterogeneous materials and biological systems [10].

The viscoelastic behavior of materials finds precise description through fractional models. The fractional Maxwell and Kelvin–Voigt models effectively capture stress–strain relationships across multiple time scales, offering superior representation of material memory effects [11]. Electromagnetic applications benefit from fractional-order models, especially

in analyzing wave propagation through complex media. These models excel at describing frequency-dependent phenomena in biological tissues and metamaterials. Control systems engineering employs fractional calculus in controller design, notably in fractional-order PID controllers, achieving improved performance for systems with hereditary characteristics. In biological applications, fractional modeling illuminates complex processes from microcirculation to cellular transport. The approach particularly suits systems exhibiting power-law behavior and memory effects [12]. The realm of quantum mechanics and structural analysis has also embraced fractional calculus, enabling advanced descriptions of quantum phenomena and thermoelastic coupling in nanostructures and composites [13].

The development of fractional calculus has its roots in the works of pioneers like Liouville and Caputo, who were influenced by the real-world applications and practical modeling capabilities offered by fractional derivatives [14]. The classical fractional derivative frameworks, such as the Riemann–Liouville and Caputo definitions, have become widely used due to their ability to describe memory-dependent and nonlocal processes in a variety of scientific and engineering disciplines [15].

In recent years, fractional calculus has been extended beyond the classical Riemann–Liouville and Caputo definitions to address new challenges in modeling real-world phenomena. Caputo and Fabrizio [16, 17] introduced a novel fractional derivative with a nonsingular exponential kernel, addressing a key limitation of traditional fractional derivatives that contained singularities in time-domain formulations.

The Atangana–Baleanu fractional derivative [18, 19] represents another significant advancement, introducing a generalized framework with a Mittag-Leffler function kernel. This derivative accounts for processes with more complex memory behaviors, effectively bridging the gap between classical fractional models and real-world dynamics. These modern approaches, featuring nonsingular and Mittag-Leffler kernels, represent a fundamental paradigm shift in fractional calculus [20].

Elastic rods are fundamental components in engineering and physics, with applications spanning from large-scale structures to micro-scale and nanoscale systems. Their behavior under axial, bending, torsional, and shear loads can be accurately described using elasticity theories. These range from classical models like Euler–Bernoulli to advanced theories incorporating viscoelastic, thermal, and nonlinear effects [21]. As technology advances, the inclusion of nonlocal and scale-dependent effects (e.g., in nanorods) is becoming increasingly important for accurate modeling and analysis of elastic rods in cutting-edge applications. At the nanoscale, elastic rod models need to account for surface effects, nonlocal elasticity, and scale-dependent behaviors [22]. The Klein–Gordon-type nonlocal elasticity is often used to incorporate internal length scale effects.

The study of moving heat sources in elastic bodies is essential in analyzing the thermoelastic behavior of materials subjected to dynamic thermal loads. This phenomenon arises in various engineering and physical applications, such as welding processes, frictional heating, laser-material interactions, and thermal shock problems [23]. A moving heat source across an elastic body generates transient temperature fields. These temperature changes induce thermal stresses and deformations in the material [24].

Moving heat source analysis plays a crucial role in numerous applications. In laser welding and machining processes, the moving heat source creates localized heating and thermal stresses, making it essential to understand the thermoelastic response for reducing

residual stresses and preventing thermal damage [25]. Similarly, in mechanical systems like brakes and clutches, frictional heating generates moving heat sources relative to rotating or sliding components, producing complex thermal gradients and stress patterns [26].

Nonlocal elasticity theory has emerged as a foundational framework in nanomechanical applications. This theory effectively addresses various phenomena, including wave propagation, composite wave dynamics, dislocation mechanics, mechanical fractures, and fluid surface tension effects [26]. Nanotubes and nanobeams have attracted significant research attention due to their unique mechanical properties and widespread applications in miniaturized systems. The theory of nonlocal elasticity continues to evolve, expanding its scope to address increasingly complex problems in nanomechanics [26, 27]. This theoretical advancement has enabled researchers to develop deeper insights into material behavior at molecular scales.

Classical continuum mechanics operates on a fundamental assumption: the stress at any point depends exclusively on the strain at that same point. However, the nonlocal theory revolutionized this perspective by recognizing that stress at a point is influenced by the stress and strain fields throughout a finite spatial region. This consideration of long-range molecular interactions and small-scale effects has proven particularly valuable in understanding nanoscale systems, where such influences are significant. Eringen [28–30] introduced the nonlocal continuum mechanics framework as a response to the limitations of classical mechanics in analyzing small-scale structures. This groundbreaking theory marked a significant departure from traditional approaches to material behavior.

Carbon nanotubes and nanobeams represent the most comprehensively studied structures within the framework of nonlocal elasticity theory. This focused attention stems from their crucial role in nanoelectromechanical systems (NEMS) and their remarkable potential in developing high-performance materials [31]. These structures serve as cornerstone elements in modern nanotechnology, offering unique combinations of mechanical, electrical, and thermal properties that make them invaluable for advanced applications.

The Klein–Gordon-type nonlocal elasticity theory represents a significant advancement in modeling nanoscale systems. This sophisticated framework builds upon Eringen's nonlocal continuum mechanics by incorporating time-dependent dynamics and scale effects into the governing equations [32]. The theory introduces both internal length and time scale effects, addressing fundamental limitations of classical elasticity when applied to small-scale structures. This enhancement is particularly crucial for nanoscale elements such as nanorods, nanobeams, and nanotubes, where traditional models fail to capture long-range interactions, size dependence, and dynamic effects [33].

The Klein–Gordon-type model excels in analyzing wave propagation, vibrations, and transient phenomena in nanostructured materials. Its practical applications are especially evident in nanomechanical systems, such as nanoresonators and nanoactuators, where it accurately predicts size-dependent natural frequencies and damping behavior. The Klein–Gordon-type nonlocal elasticity theory incorporates two essential parameters that work together to provide comprehensive modeling capabilities at the nanoscale [34].

The internal length scale parameter plays a fundamental role in capturing size-dependent behavior in nanostructures, addressing a critical limitation of classical elasticity theory [35]. This element enables the accurate representation of mechanical properties that

vary with the physical dimensions of nanoscale structures, a phenomenon that traditional elasticity approaches cannot describe. The time scale parameter complements the spatial component by accounting for dynamic effects in nanostructures [36]. This aspect is particularly crucial for modeling wave dispersion and relaxation processes, making the theory well-suited for analyzing transient and high-frequency problems. Through the combined action of these spatial and temporal parameters, the theory provides a robust framework for understanding the complete mechanical behavior at molecular scales [37, 38].

The classical Fourier heat conduction model, despite its widespread use, suffers from inherent limitations. Its assumption of infinite heat transfer speeds implies that thermal disturbances propagate instantaneously through a medium, which directly contradicts the principle of causality. This limitation becomes particularly problematic when analyzing small-scale phenomena or in systems subject to high heat fluxes, where the rate of heat transfer cannot be considered infinite. Such scenarios require more accurate models that account for the finite speed of thermal wave propagation. This is a crucial consideration for understanding thermal behavior in advanced materials and nanoscale systems [39].

To address these theoretical shortcomings, researchers have developed several advanced models. Notable among these are the Lord–Shulman theory [40] and the dual-phase lag (DPL) model [41, 42]. These modifications incorporate crucial physical considerations, including finite propagation speeds and small-scale effects. The dual-phase lag model, when coupled with nonlocal continuum mechanics, offers a particularly robust framework for studying thermoelastic behavior in nanoscale systems [43]. This advanced approach successfully addresses the limitations of classical theories by incorporating three key elements: finite heat propagation speeds, memory effects, and size-dependent phenomena. These features make it especially valuable for analyzing thermal behavior at the nanoscale [44].

Numerous investigations have greatly enhanced our understanding of piezoelectric materials and structures, leading to the development of advanced models for examining their thermoelastic and dynamic behaviors. Guo *et al.* [45] introduced a groundbreaking nonlocal piezoelectric thermoelasticity theory that incorporates Eringen-type nonlocal single phase lag heat conduction. Their study focused on the transient thermo-electromechanical responses of piezoelectric nanorods, shedding light on how these materials react under different thermal and mechanical circumstances. In another contribution, Guo *et al.* [46] also crafted a fractional-order rate-dependent piezoelectric thermoelasticity theory utilizing new fractional derivatives. This framework was applied to study the transient structural responses of smart piezoelectric composite laminates, taking into account the impact of imperfect interfacial conditions and the variances in material property ratios on wave behavior and structural responses.

Li *et al.* [47] presented a fractional-order rate-dependent thermoelastic diffusion theory, employing new fractional derivatives with nonsingular kernels, to analyze the transient dynamic responses of sandwich-like composite laminates. Their work provided a thorough understanding of how these materials behave under thermal and mechanical loads. Furthermore, Li *et al.* [48] investigated the size-dependent thermo-electromechanical responses of multi-layered piezoelectric nanoplates, emphasizing their potential applications in vibration control. They focused on the influence of size and material properties on the vibration characteristics of these nanoplates. Lastly, Li *et al.* [49] proposed a non-Fick diffusion-elasticity model rooted in a novel nonlocal dual phase lag diffusion approach.

This innovative model was utilized to explore the transient dynamic responses of materials, offering valuable insights into their behavior under diverse loading scenarios.

This paper introduces a novel framework for analyzing magneto-thermoelastic interactions in rotating viscoelastic nanorods subjected to moving heat sources, representing a significant advancement in the modeling of nanoscale systems. The core innovation lay in the integration of the Klein–Gordon-type nonlocal elasticity theory, which incorporated internal length and time scale effects into the governing equations to accurately capture small-scale interactions. Additionally, a fractional heat conduction model employing two-parameter tempered-Caputo derivatives introduced memory effects and nonlocal heat conduction, ensuring finite thermal wave speeds and addressing the limitations of classical Fourier models. Furthermore, the model incorporated the Kelvin–Voigt viscoelastic framework, which accounted for energy dissipation due to the viscoelastic behavior of the material, thereby enhancing its predictive capabilities and realism.

What distinguishes this work is the unique combination of rotation, viscoelasticity, magnetic forces, and fractional heat conduction, resulting in a highly coupled and nonlinear problem. This comprehensive formulation successfully captures the intricate interactions among thermal, mechanical, and magnetic fields in nanorods. The inclusion of uniform rotational motion under a primary magnetic field introduces additional complexities, such as Lorentz forces, centrifugal effects, and Coriolis forces, which significantly influence the system's dynamics. The proposed model systematically addresses all these phenomena, providing a robust framework for understanding and predicting the behavior of nanoscale systems in dynamic environments.

Numerical simulations validate the model's capability to accurately predict the dynamic behavior of nanorods under the combined effects of thermal, mechanical, and magnetic influences. The results underscore several critical insights—the integration of fractional-order heat conduction, nonlocal elasticity, and viscoelastic damping are indispensable for achieving realistic and reliable thermal and mechanical responses. This study establishes a robust theoretical framework for the design and optimization of advanced nanoscale devices, including nanoactuators, thermal sensors, and magneto-mechanical systems, tailored to operate in complex and dynamic environmental conditions.

2 Formulation of fractional space-time nonlocal thermoelasticity theory

The theory of fractional spacetime nonlocal thermoelasticity presents an advanced mathematical framework that goes beyond conventional thermoelastic models. This intricate approach merges two influential mathematical ideas: nonlocal effects and fractional operators applicable in both spatial and temporal domains. By integrating these components, the model effectively addresses key limitations found in classical thermoelasticity. This all-encompassing framework is particularly beneficial for examining materials at nanoscale and microscale levels, where standard methods often struggle to account for vital behaviors. At these scales, materials display complex phenomena such as long-range molecular interactions, enduring memory effects, and unusual thermal and mechanical responses. The fractional spacetime framework adeptly models these sophisticated behaviors, equipping researchers with powerful tools to understand and predict material responses that traditional models may not fully capture.

The nonlocal elasticity theory extends classical elasticity by considering that the stress tensor at a given point $\boldsymbol{r}$ in a nanomaterial is influenced not only by the strain at that

point but also by the strain at all other points within the body. This principle is particularly crucial for studying the mechanical and thermal behavior of nanostructures, where size effects and long-range interactions become significant. To address these complex interactions, the theoretical formulation combines nonlocal elasticity, viscoelasticity, and thermoelasticity to describe the dynamic behavior of nanomaterials.

The nonlocal stress tensor $\tau_{kl}(\boldsymbol{r})$ in a nonlocal elastic medium is expressed as follows [28–30]:

$$\tau_{kl}(\boldsymbol{r}) = \int_V K\left(\left|\boldsymbol{r}' - \boldsymbol{r}\right|, \xi\right) \sigma_{kl}\left(\boldsymbol{r}'\right) \mathrm{d}V\left(\boldsymbol{r}'\right). \tag{1}$$

In Eq. (1), the nonlocal kernel function $K\left(\left|\boldsymbol{r}' - \boldsymbol{r}\right|, \xi\right)$ characterizes the influence of strain at point $\boldsymbol{r}$ on the stress at point $\boldsymbol{r}'$. The nonlocal parameter ξ is defined by the material constant e_0, which is determined experimentally, and the internal characteristic length a (such as lattice spacing or grain size) along with the external characteristic length l (representing the overall dimensions of the structure). The macroscopic stress tensor at point $\boldsymbol{r}'$ is denoted as $\sigma_{kl}\left(\boldsymbol{r}'\right)$, and V refers to the volume of the material.

For a Kelvin–Voigt viscoelastic medium, the macroscopic stress tensor $\boldsymbol{\sigma}\left(\boldsymbol{r}'\right)$ is given by [50, 51]

$$\sigma_{kl}\left(\boldsymbol{r}'\right) = \lambda_e\left(1 + \lambda_0\frac{\partial}{\partial t}\right)\varepsilon_{mm}\delta_{kl} + 2\mu_e\left(1 + \mu_0\frac{\partial}{\partial t}\right)\varepsilon_{kl} - \gamma_e\left(1 + \gamma_0\frac{\partial}{\partial t}\right)\theta\left(\boldsymbol{r}'\right)\delta_{kl}. \tag{2}$$

In this context, the strain tensor is indicated as ε_{kl}, while the temperature changes from the reference temperature T_0 is given by $\theta = T - T_0$. Key material constants include Lame's constants λ and μ as well as the viscoelastic relaxation times λ_0 and μ_0. The thermal expansion coefficient is denoted by α_t. The thermoelastic coupling parameter is defined as $\gamma_e = (3\lambda_e + 2\mu_e)\alpha_t$, and the thermo-viscoelastic relaxation parameter is expressed as $\gamma_0 = (3\lambda_e\lambda_0 + 2\mu_e\mu_0)\alpha_t/\gamma_e$.

The strain tensor ε_{kl} is defined as [52]

$$2\varepsilon_{kl} = \frac{\partial u_k}{\partial x_l} + \frac{\partial u_l}{\partial x_k}, \tag{3}$$

where u_k are the components of the displacement vector.

In the nonlocal elasticity framework, which incorporates both spatial and temporal effects, the stress tensor $\tau_{kl}(r,t)$ at a specific point r and time t is influenced not only by the strain at that point but also by the strain at other locations within the material and at earlier times. This framework effectively captures the memory effect inherent in the system, highlighting how previous states influence the current stress state. The nonlocal stress tensor can be expressed as [53]

$$\tau_{kl}(r,t) = \int_{-\infty}^{t}\int_V \mathcal{K}\left(\left|r - \hat{r}\right|, t - \hat{t}\right)\sigma_{kl}\left(\hat{r},\hat{t}\right)\mathrm{d}V\left(\hat{x}\right)\mathrm{d}\hat{t}, \tag{4}$$

where $\mathcal{K}\left(\left|r - \hat{r}\right|, t - \hat{t}\right)$ is the nonlocal elasticity tensor, and $\epsilon\sigma_{kl}\left(\hat{r},\hat{t}\right)$ represents the local stress at the point $\hat{r}$ and time $\hat{t}$. This integral formulation accounts for the spatial and temporal nonlocal interactions, incorporating the effects of past strains and distant regions on the stress state at (r,t).

Formulation (4) inherently couples both spatial nonlocality, represented by the distance $|r-\hat{r}|$, and temporal nonlocality, represented by the time difference $t-\hat{t}$. This coupling allows the stress at a given point r and time t to depend not only on the local strain but also on strains at other spatial locations and previous times. By incorporating both spatial and temporal dependencies, this formulation captures the memory effects and the influence of past events on the current stress state, which is crucial for accurately modeling complex materials and systems at small scales.

Based on the principles of nonlocal elasticity, the nonlocal stress tensor can be related to the local stress tensor as follows [52]:

$$\left(1-\ell^2\nabla^2+\tau^2\frac{\partial^2}{\partial t^2}\right)\tau_{kl}=\sigma_{kl}\left(\boldsymbol{r}'\right). \tag{5}$$

This represents a Klein–Gordon type equation that incorporates both spatial and temporal nonlocality. The equation of motion in the Klein–Gordon type nonlocal elasticity framework, which includes body forces as functions of temperature and displacement, is given by

$$\begin{aligned}&\lambda_e\left(1+\lambda_0\frac{\partial}{\partial t}\right)\frac{\partial^2 u_l}{\partial x_l x_k}+\mu_e\left(1+\mu_0\frac{\partial}{\partial t}\right)\frac{\partial^2 u_k}{\partial x_l^2}\\&\quad+\left(\lambda_e+\mu_e+\left(\lambda_e\lambda_0+\mu_e\mu_0\right)\frac{\partial}{\partial t}\right)\frac{\partial^2 u_k}{\partial x_k^2}-\gamma_e\left(1+\gamma_0\frac{\partial}{\partial t}\right)\frac{\partial\theta}{\partial x_k}\\&=\rho\left(1-\ell^2\nabla^2+\tau^2\frac{\partial^2}{\partial t^2}\right)\frac{\partial^2 u_k}{\partial t^2}+\left(1-\ell^2\nabla^2+\tau^2\frac{\partial^2}{\partial t^2}\right)F_k.\end{aligned} \tag{6}$$

The DPL model [41–44] marks a significant advancement in thermal transport theory. Unlike classical Fourier heat conduction theory, which relies on simplistic assumptions about heat propagation, the DPL model introduces important refinements by incorporating relaxation time parameters for both heat flux and temperature gradient. This development addresses a major limitation of Fourier's theory, i.e., the unrealistic assumption of infinite heat propagation speeds.

The theoretical development of thermal transport progressed through several key stages, with the Cattaneo–Vernotte model playing a pivotal role. This intermediate model introduced a single relaxation time parameter (τ_q) for heat flux, establishing the concept of finite propagation speeds. The DPL model built upon this by incorporating two separate relaxation times (τ_q and τ_θ), providing a more robust framework for understanding thermal transport. The dual-parameter approach is particularly valuable for analyzing transient conditions and high-rate thermal processes, where classical theories fail to offer accurate predictions. In the context of the DPL model, a generalized form of Fourier's law can be expressed as follows: [43, 44]:

$$q_i+\tau_q\frac{\partial q_i}{\partial t}=-K\left(\theta_{,i}+\tau_\theta\frac{\partial\theta_{,i}}{\partial t}\right), \tag{7}$$

where $q_i\left(\boldsymbol{r},t\right)$ is the heat flux vector and K is the thermal conductivity.

Equation (7) ensures that both heat flux and temperature gradients exhibit time delays, accurately reflecting more realistic thermal behavior. The energy balance equation, which

links heat transport to mechanical effects, is given by [53]

$$\rho C_E \frac{\partial \theta}{\partial t} + T_0 \gamma_e \left(1 + \gamma_0 \frac{\partial}{\partial t}\right) \frac{\partial \varepsilon_{mm}}{\partial t} = -q_{i,i} + Q, \tag{8}$$

where C_E denotes the specific heat capacity of the material and Q represents the internal energy input into the system.

In materials science, the Caputo tempered fractional derivative has become a powerful tool for modeling complex thermal dynamics and mechanical interactions that surpass the capabilities of standard fractional derivatives. It is especially effective for describing processes that exhibit memory effects, long-range interactions, and the gradual decay of past influences over time, making it highly suitable for advanced materials subjected to various thermal and mechanical conditions. The Caputo tempered fractional derivative is an extension of the Caputo fractional derivative, incorporating an exponential tempering factor. This factor modifies memory effects by adjusting the impact of past states on the system's current behavior. This modification offers a more flexible and realistic framework for modeling materials with time-dependent interactions and gradually diminishing correlations.

The Caputo fractional derivative is characterized by the definition [54]

$${}_0^C D_0^{(\alpha)} Y(t) = \frac{1}{\Gamma(1-\alpha)} \int_0^t \frac{1}{(t-\vartheta)^\alpha} \frac{d}{d\vartheta} Y(\vartheta)\, d\vartheta. \tag{9}$$

The Caputo tempered (CT) fractional derivative, represented as ${}_0^{CT} D_t^{\alpha,\chi}$, is defined as follows [55]:

$${}_0^{CT} D_t^{\alpha,\chi} Y(t) = \frac{e^{-\chi t}}{\Gamma(1-\alpha)} \int_0^t \frac{d}{d\vartheta} \left(e^{\chi \xi} Y(\vartheta)\right) (t-\vartheta)^{-\alpha}\, d\xi, \quad \alpha \in (0,1). \tag{10}$$

In this context, $\alpha \in (0,1)$ signifies the order of the derivative, reflecting the degree of the memory effect present in the system. The parameter $\chi > 0$ acts as the tempering parameter, adjusting the strength of this memory effect. Furthermore, $\Gamma(1-\alpha)$ denotes the gamma function, which is employed to maintain appropriate normalization in the formulation.

The derivative retains the long-term memory effects typical of standard fractional derivatives. However, the tempering factor $e^{-\chi t}$ lessens the influence of previous states, allowing for a more precise depiction of processes where memory effects decline over time [56]. This modification facilitates a more realistic modeling of dynamic behaviors across diverse systems. It proves especially beneficial for processes that display fading memory effects, like thermal relaxation in materials.

The Laplace transform of the Caputo tempered fractional derivative streamlines its application in solving differential equations. For any function $Y(t)$ with initial conditions given by $Y(0)$, the Laplace transform is expressed as [57]

$$\mathcal{L}\left[D_t^{(\alpha)} Y(t)\right] = (s+\chi)^\alpha \mathcal{L}[Y(t)] - (s+\chi)^{\alpha-1} Y(0). \tag{11}$$

By integrating the CT fractional derivative into the DPL model, the generalized heat conduction law is formulated as [58]

$$\left(1+\tau_q^{\alpha}D_t^{(\alpha)}\right)q_i=-K\left(1+\tau_\theta^{\alpha}D_t^{(\alpha)}\right)\theta_{,i}. \tag{12}$$

Merging Eq. (12) with the energy balance Eq. (8) results in the fractional heat transport equation [59]

$$\left(1+\tau_q^{\alpha}D_t^{(\alpha)}\right)\left[\rho C_E\frac{\partial\theta}{\partial t}+T_0\gamma_e\left(1+\gamma_0\frac{\partial}{\partial t}\right)\frac{\partial\varepsilon_{mm}}{\partial t}-Q\right]=K\left(1+\tau_\theta^{\alpha}D_t^{(\alpha)}\right)\theta_{,ii}. \tag{13}$$

This equation captures the interaction of fractional memory, limited propagation speeds, and thermal-mechanical coupling in thermoelastic systems.

In thermoelastic solids, the effect of electromagnetic fields is incorporated through Maxwell's equations, which detail the interactions between electric and magnetic fields and matter. The governing equations can be represented as follows [60]:

$$\begin{aligned}&\overrightarrow{J}=\nabla\times\overrightarrow{h},\nabla\times\overrightarrow{E}=-\mu_0\frac{\partial\overrightarrow{h}}{\partial t},\overrightarrow{J}=\sigma_0\left(\overrightarrow{E}+\mu_0\left(\frac{\partial\overrightarrow{u}}{\partial t}\times\overrightarrow{H}\right)\right),\\&\overrightarrow{h}=\nabla\times\left(\overrightarrow{u}\times\overrightarrow{H}\right),\nabla\cdot\overrightarrow{h}=0.\end{aligned} \tag{14}$$

In this context, $\overrightarrow{J}$ signifies the current density vector, whereas $\overrightarrow{E}$ represents the electric displacement vector. The complete magnetic field is expressed as $\overrightarrow{H}=\overrightarrow{h}+\overrightarrow{H}_0$, where $\overrightarrow{h}$ is the induced magnetic field and $\overrightarrow{H}_0$ is the initial uniform magnetic field. Furthermore, σ_0 denotes electrical conductivity, while μ_0 refers to magnetic permeability. Together, these variables characterize the electromagnetic properties and interactions occurring within the system

When a thermoelastic medium rotates at a steady angular velocity $\overrightarrow{\Omega}=\Omega\overrightarrow{n}$, where $\overrightarrow{n}$ is the unit vector aligned with the rotation axis, it becomes important to factor in the effects of centripetal acceleration and Coriolis force within the governing equations. These rotational influences significantly affect the thermoelastic characteristics of the medium, altering the stress, strain, and displacement fields, while also impacting the heat conduction process [61]. As a result, a thorough understanding of these dynamics is essential for accurately modeling the behavior of rotating thermoelastic systems. In a rotating frame, the inertial forces consist of centripetal acceleration and the Coriolis force. Centripetal acceleration, which is proportional to Ω^2, acts outward radially and is represented by the expression $\overrightarrow{\Omega}\times\left(\overrightarrow{\Omega}\times\overrightarrow{u}\right)$, with $\overrightarrow{u}$ being the displacement vector. The Coriolis force, which results from rotation and is proportional to Ω, acts at a right angle to the direction of motion and is expressed as $2\overrightarrow{\Omega}\times\overrightarrow{\dot{u}}$, where $\overrightarrow{\dot{u}}$ signifies the velocity vector [62]. For a rotating medium with angular velocity Ω, extra terms accounting for centripetal acceleration and Coriolis forces are incorporated into the equation of motion [54, 63]:

$$\begin{aligned}&\lambda_e\left(1+\lambda_0\frac{\partial}{\partial t}\right)\frac{\partial^2u_l}{\partial x_lx_k}+\mu_e\left(1+\mu_0\frac{\partial}{\partial t}\right)\frac{\partial^2u_k}{\partial x_l^2}\\&\quad+\left(\lambda_e+\mu_e+(\lambda_e\lambda_0+\mu_e\mu_0)\frac{\partial}{\partial t}\right)\frac{\partial^2u_k}{\partial x_k^2}-\gamma_e\left(1+\gamma_0\frac{\partial}{\partial t}\right)\frac{\partial\theta}{\partial x_k}\end{aligned} \tag{15}$$

$$= \rho \left(1 - \ell^2 \nabla^2 + \tau^2 \frac{\partial^2}{\partial t^2}\right) \frac{\partial^2 u_k}{\partial t^2} + \left(1 - \ell^2 \nabla^2 + \tau^2 \frac{\partial^2}{\partial t^2}\right) F_k$$
$$\times \rho \left(1 - \ell^2 \nabla^2 + \tau^2 \frac{\partial^2}{\partial t^2}\right) \left[\ddot{\vec{u}} + \vec{\Omega} \times \left(\vec{\Omega} \times \vec{u}\right) + \left(2\vec{\Omega} \times \dot{\vec{u}}\right)\right]_k .$$

3 Problem formulation for nonlocal visco-thermoelastic rotating rod

This problem addresses a homogeneous, isotropic nonlocal visco-thermoelastic finite rod that is initially unstressed, unstrained, and uniformly maintained at a temperature T_0. As depicted in Fig. 1, the rod rotates around the z-axis with a constant angular velocity $\vec{\Omega} = (0, 0, \Omega)$, while the x-axis indicates the rod's axial direction. A moving heat source $Q(x, t)$ is introduced at $x = 0$ and travels along the axial direction (x) of the rod. The coupled thermoelastic behavior takes into account the influences of nonlocal elasticity, fractional heat conduction, viscoelasticity, rotation, and the presence of an applied magnetic field. The analysis also involves several key assumptions: it is treated as one-dimensional, with the fields depending only on the spatial coordinate x and time t. Displacement is restricted to the axial direction, represented as $u_x = u(x, t)$, while u_y and u_z remain zero.

Furthermore, the rod is exposed to a magnetic field $\vec{H} = (0, H_x, 0)$, which is oriented perpendicular to the axis of the rod. The presence of this longitudinal magnetic field $\vec{H}$ results in a Lorentz force $\vec{F} = \vec{J} \times \vec{H}$, where $\vec{J}$ denotes the current density. The components of this force are as follows:

$$\vec{F} = (f_x, f_y, f_z) = -\sigma_0 \mu_0 H_x^2 \left(\frac{\partial u}{\partial t}, 0, 0\right). \tag{16}$$

The nonlocal stress tensor for the rod is determined by the principles of nonlocal elasticity theory. By incorporating the strain tensor into the nonlocal stress equation, the axial stress τ_{xx} is formulated as follows:

$$\left(1 - \ell^2 \frac{\partial^2}{\partial x^2} + \tau^2 \frac{\partial^2}{\partial t^2}\right) \tau_{xx}$$
$$= \left(\lambda_e + 2\mu_e + (\lambda_e \lambda_0 + 2\mu_e \mu_0) \frac{\partial}{\partial t}\right) \frac{\partial u}{\partial x} - \gamma_e \left(1 + \gamma_0 \frac{\partial}{\partial t}\right) \theta. \tag{17}$$

The rod's equation of motion is obtained by inserting the nonlocal stress tensor (Eq. (17)) and the Lorentz force (Eq. (16)) into the linear momentum balance equation. This results

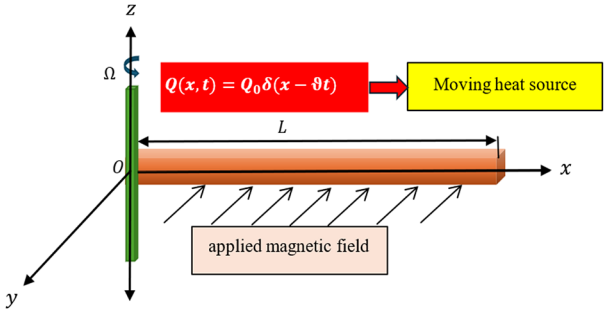

Figure 1 Schematic representation of the nonlocal thermo-viscoelastic finite rod

in the following expression:

$$\begin{aligned}&\left(\lambda_e+2\mu_e+\left(\lambda_e\lambda_0+2\mu_e\mu_0\right)\frac{\partial}{\partial t}\right)\frac{\partial^2 u}{\partial x^2}-\gamma_e\left(1+\gamma_0\frac{\partial}{\partial t}\right)\frac{\partial\theta}{\partial x}\\&=\left(1-\ell^2\frac{\partial^2}{\partial x^2}+\tau^2\frac{\partial^2}{\partial t^2}\right)\left[\rho\frac{\partial^2 u}{\partial t^2}+\rho\Omega^2 u+\sigma_0\mu_0 H_x^2\frac{\partial u}{\partial t}\right].\end{aligned}\tag{18}$$

Heat transfer within the rod is described by the generalized fractional heat equation, which utilizes Caputo tempered fractional time derivatives to incorporate memory effects. The heat equation can be expressed as follows:

$$K\left(1+\tau_\theta^\alpha D_t^{(\alpha)}\right)\frac{\partial^2\theta}{\partial x^2}=\left(1+\tau_q^\alpha D_t^{(\alpha)}\right)\left[\rho C_E\frac{\partial\theta}{\partial t}+T_0\gamma_e\left(1+\gamma_0\frac{\partial}{\partial t}\right)\frac{\partial^2 u}{\partial t\partial x}-Q\right].\tag{19}$$

The governing equations can be streamlined by applying specific nondimensional variables to scale them appropriately. These variables usually encompass scale factors for displacement, time, temperature, and other pertinent physical properties. This process of dimensionalization simplifies the analysis of the system's dynamics by reducing the number of parameters involved and enabling easier comparisons under various conditions. The primary nondimensional variables are defined as follows:

$$\begin{aligned}&\left\{x',u'\right\}=c_0\omega_0\left\{x,u\right\},\left\{t',\tau_\theta',\tau_q',\tau'\right\}=c_0^2\omega_0\left\{t,\tau_\theta,\tau_q,\tau\right\},\ell'=c_0^2\omega_0^2\ell,\\&\Omega'=\frac{\Omega}{c_0^2\omega_0},\theta'=\frac{\theta}{T_0},\tau_{xx}'=\frac{\tau_{xx}}{\lambda_e+2\mu_e},Q'=\frac{Q}{KT_0c_0^2\omega_0^2},c_0^2=\frac{\left(\lambda_e+2\mu_e\right)}{\rho},\omega_0=\frac{\rho C_E}{K}.\end{aligned}\tag{20}$$

Here, c_0 represents the speed of longitudinal elastic waves, while ω_0 denotes the speed of thermal waves. For simplicity, we can omit the primes, allowing us to express the nondimensional field equations in the following manner:

$$\left(1-\ell^2\frac{\partial^2}{\partial x^2}+\tau^2\frac{\partial^2}{\partial t^2}\right)\tau_{xx}=\left(1+\beta_1^2\frac{\partial}{\partial t}\right)\frac{\partial u}{\partial x}-b\left(1+\beta_0^2\frac{\partial}{\partial t}\right)\theta,\tag{21}$$

$$\left(1-\ell^2\frac{\partial^2}{\partial x^2}+\tau^2\frac{\partial^2}{\partial t^2}\right)\left[\frac{\partial^2 u}{\partial t^2}+\Omega^2 u+\varepsilon\frac{\partial u}{\partial t}\right]=\left(1+\beta_1^2\frac{\partial}{\partial t}\right)\frac{\partial^2 u}{\partial x^2}-b\left(1+\beta_0^2\frac{\partial}{\partial t}\right)\frac{\partial\theta}{\partial x},\tag{22}$$

$$\left(1+\tau_\theta^\alpha D_t^{(\alpha)}\right)\frac{\partial^2\theta}{\partial x^2}=\left(1+\tau_q^\alpha D_t^{(\alpha)}\right)\left[\frac{\partial\theta}{\partial t}+g\left(1+\beta_0^2\frac{\partial}{\partial t}\right)\frac{\partial^2 u}{\partial t\partial x}-Q\right],\tag{23}$$

where

$$\begin{aligned}&\beta_1^2=\frac{c_0^2\omega_0\left(\lambda_e\lambda_0+2\mu_e\mu_0\right)}{\lambda_e+2\mu_e},b=\frac{\gamma_e T_0}{\lambda_e+2\mu_e},\\&\beta_0^2=c_0^2\omega_0\gamma_0,\varepsilon=\frac{\sigma_0\mu_0 H_x^2}{\rho c_0^2\omega_0},g=\frac{\gamma_e}{\rho C_E}.\end{aligned}\tag{24}$$

In this context, ε refers to the magnetic field coupling parameter. The initial conditions are defined as follows:

$$\theta\left(x,0\right)=\frac{\partial\theta\left(x,0\right)}{\partial t}=0,u\left(x,0\right)=\frac{\partial u\left(x,0\right)}{\partial t}=0,\tau_{xx}\left(x,0\right)=\frac{\partial\tau_{xx}\left(x,0\right)}{\partial t}=0.\tag{25}$$

The boundary conditions describe a rod that is thermally insulated at both ends, indicating that heat cannot flow across the boundaries. Furthermore, one end of the rod is securely fixed, while the opposite end is unrestrained by axial stress, permitting thermal expansion to occur freely.

At the first end, where $x = 0$, the rod is anchored in place, which results in the displacement being zero:

$$u(x,t) = 0 \quad \text{at} \quad x = 0. \tag{26}$$

At end $x = \mathrm{L}$, the rod is free from axial stress. This implies that the axial stress τ_{xx} vanishes at the free end, which translates to

$$\tau_{xx}(x,t) = 0 \quad \text{at} \quad x = L. \tag{27}$$

The boundaries ($x = 0$ and $x = \mathrm{L}$) are thermally insulated, which means there is no heat transfer across them. Mathematically, this condition implies that the heat flux vanishes at both ends:

$$K\frac{\partial\theta(x,t)}{\partial x} = 0 \quad \text{on} \quad x = 0, L. \tag{28}$$

The rod experiences the influence of a moving heat source $Q(x,t)$ with a steady strength denoted as Q_0, which consistently emits energy while advancing along the positive x-axis at a constant speed ϑ. This heat source is represented as a Dirac delta function $\delta(x - \vartheta t)$, simulating a point heat source navigating through the rod. The nondimensionalized version of the heat source can be articulated as follows [63, 64]:

$$Q(x,t) = Q_0\delta(x - \vartheta t). \tag{29}$$

The Dirac delta function $\delta(x - \vartheta t)$ guarantees that the heat source is focused at a specific location $x = \vartheta t$ at any moment t. This kind of heat source is widely utilized in simulations of localized heating phenomena, such as those occurring during laser heating or frictional heating processes.

4 Laplace transform solution

The Laplace transform method is employed to obtain explicit solutions for the governing equations of a nonlocal visco-thermoelastic rod. This technique translates the equations from the time domain into the Laplace domain, making the process of finding solutions more straightforward. The Laplace transform of a function $f(x,t)$ can be expressed as follows:

$$\overline{f}(x,t) = \int_0^\infty f(x,t)\, e^{-st} dt. \tag{30}$$

The governing equations in the Laplace transform domain, incorporating the initial conditions, can be articulated as follows:

$$\left(1 - \ell^2\frac{d^2}{dx^2} + \tau^2 s^2\right)\overline{\tau}_{xx} = \left(1 + \beta_1^2 s\right)\frac{\mathrm{d}\overline{u}}{\mathrm{d}x} - b\left(1 + \beta_0^2 s\right)\overline{\theta}, \tag{31}$$

$$\alpha_0 \left(1 - \ell^2 \frac{d^2}{dx^2} + \tau^2 s^2\right) \overline{u} = \left(1 + \beta_1^2 \mathrm{s}\right) \frac{\mathrm{d}^2 \overline{u}}{\mathrm{d}x^2} - b \left(1 + \beta_0^2 s\right) \frac{\mathrm{d}\overline{\theta}}{\mathrm{d}x}, \tag{32}$$

$$\frac{\mathrm{d}^2 \overline{\theta}}{\mathrm{d}x^2} = \frac{\left(1 + \tau_q^\alpha \Lambda\right)}{\left(1 + \tau_\theta^\alpha \Lambda\right)} \left[s\overline{\theta} + \mathrm{sg} \left(1 + \beta_0^2 \mathrm{s}\right) \frac{\mathrm{d}\overline{u}}{\mathrm{d}x} - \frac{Q_0}{\vartheta} e^{-(s/\vartheta)x} \right], \tag{33}$$

where $\alpha_0 = s^2 + \Omega^2 + \varepsilon s$ and

$$\Lambda = \begin{cases} \mathrm{s}^\alpha & \text{for C fractional operotor,} \\ (\mathrm{s} + \chi)^\alpha & \text{for CT fractional operotor.} \end{cases} \tag{34}$$

By substituting $\overline{\theta}$ from Eq. (32) into Eq. (33), the equation for $\overline{u}$ becomes

$$\left(\frac{\mathrm{d}^4}{\mathrm{d}x^4} - m_1 \frac{\mathrm{d}^2}{\mathrm{d}x^2} + m_2 \right) \overline{u}(x, s) = m_3 e^{-(s/\vartheta)x}, \tag{35}$$

where the coefficients m_1, m_2, and m_3 are defined as follows:

$$m_1 = \alpha_4 + \frac{\alpha_7}{\alpha_1} + \frac{\alpha_3 \alpha_5}{\alpha_1}, m_2 = \frac{\alpha_7 \alpha_4}{\alpha_1}, m_3 = \frac{s\alpha_3 \alpha_6}{\vartheta \alpha_1}. \tag{36}$$

Also, the intermediate quantities α_i are given by

$$\begin{aligned} &\alpha_1 = \left(1 + \beta_1^2 \mathrm{s}\right) + \ell^2 \alpha_0, \alpha_2 = s^2 + \mathrm{s}\varepsilon + \Omega^2, \alpha_3 = b \left(1 + \beta_0^2 s\right), \\ &\alpha_4 = \frac{s \left(1 + \tau_q^\alpha \Lambda\right)}{\left(1 + \tau_\theta^\alpha \Lambda\right)}, \alpha_5 = g\alpha_4 \left(1 + \beta_0^2 s\right), \alpha_6 = \frac{\alpha_4 \mathrm{Q}_0}{s\vartheta}, \alpha_7 = \alpha_0 \left(1 + + \tau^2 s^2\right). \end{aligned} \tag{37}$$

The general solution to the fourth-order differential equation (35) can be expressed as

$$\overline{u}\,(x, s) = \sum_{n=1}^{2} \left(C_n \mathrm{e}^{-k_n x} + C_{n+2} \mathrm{e}^{k_n x} \right) + C_5 e^{-(s/\vartheta)x}, \tag{38}$$

where k_1 and k_2 are the roots of the characteristic equation

$$k^4 - m_1 k^2 + m_2 = 0. \tag{39}$$

The parameters C_n $(n = 1, 2, 3, 4)$ are constants determined from the boundary conditions, and the parameter C_5 is given by

$$C_5 = \frac{m_3}{(s/\vartheta)^4 - m_1 (s/\vartheta)^2 + m_2}. \tag{40}$$

Similarly, by eliminating $\overline{u}$ from Eq. (32) and Eq. (33), the governing equation for $\overline{\theta}$ becomes

$$\left(\frac{\mathrm{d}^4}{\mathrm{d}x^4} - m_1 \frac{\mathrm{d}^2}{\mathrm{d}x^2} + m_2 \right) \overline{\theta}(x) = m_4 e^{-(s/\vartheta)x}, \tag{41}$$

where $m_4 = \frac{\alpha_7 \alpha_6}{\alpha_1} - \frac{s^2 \alpha_6}{\vartheta^2}$.

The general solution for $\overline{\theta}$ can be expressed as

$$\overline{\theta}(x,s) = \sum_{n=1}^{2} \left(\beta_n C_n \mathrm{e}^{-k_n x} + \beta_{n+2} C_{n+2} \mathrm{e}^{k_n x}\right) + C_6 e^{-(s/\vartheta)x}, \tag{42}$$

where β_n and β_{n+2} $(n = 1, 2)$ are given by

$$\begin{aligned}
\beta_n &= -\frac{\alpha_1 k_n^2 - \alpha_7}{\alpha_3 k_n}, \quad n = 1, 2, \\
\beta_{n+2} &= \frac{\alpha_1 k_n^2 - \alpha_7}{\alpha_3 k_n}, \quad n = 1, 2, \\
C_6 &= \frac{m_4}{(s/\vartheta)^4 - m_1 (s/\vartheta)^2 + m_2}.
\end{aligned} \tag{43}$$

The expression for the nonlocal thermal stress $\overline{\tau}_{xx}(x,s)$ is derived by substituting $\overline{u}(x,s)$ (Eq. (38)) and $\overline{\theta}(x,s)$ (Eq. (42)) into the nonlocal stress-strain relation, Eq. (31):

$$\overline{\tau}_{xx}(x,s) = \sum_{n=1}^{2} \left(-\gamma_n C_n \mathrm{e}^{-k_n x} + \gamma_{n+2} C_{n+2} \mathrm{e}^{k_n x}\right) + C_7 e^{-(s/\vartheta)x}, \tag{44}$$

where the coefficients γ_n, γ_{n+2}, and C_7 are defined as follows:

$$\begin{aligned}
\gamma_n &= -\frac{\left(1 + \beta_1^2 s\right) k_n + b\left(1 + \beta_0^2 s\right) \beta_n}{1 - \ell^2 k_n^2 + \tau^2 s^2}, \quad n = 1, 2, \\
\gamma_{n+2} &= \frac{\left(1 + \beta_1^2 s\right) k_n - b\left(1 + \beta_0^2 s\right) \beta_n}{1 - \ell^2 k_n^2 + \tau^2 s^2}, \quad n = 1, 2, \\
C_7 &= \frac{-C_5\left(1 + \beta_1^2 s\right)\left(\frac{s}{\vartheta}\right) - b\left(1 + \beta_0^2 s\right) C_6}{1 - \ell^2 (s/\vartheta)^2 + \tau^2 s^2}.
\end{aligned} \tag{45}$$

The boundary conditions (26)–(28) in the Laplace domain are:

$$\begin{aligned}
&\overline{u}(0,s) = 0, \quad \overline{\tau}_{xx}(0,s) = 0, \\
&\frac{\partial \overline{\theta}(0,s)}{\partial x} = 0, \quad \frac{\partial \overline{\theta}(L,s)}{\partial x} = 0.
\end{aligned} \tag{46}$$

By substituting Eqs. (38), (42), and (44) into the aforementioned boundary conditions, we derive the following four linear equations:

$$\sum_{n=1}^{2} (C_n + C_{n+2}) = -C_5, \tag{47}$$

$$\sum_{n=1}^{2} k_n \left(C_n \mathrm{e}^{-k_n L} - C_{n+2} \mathrm{e}^{k_n L}\right) = C_5 e^{-(s/\vartheta)L}, \tag{48}$$

$$\sum_{n=1}^{2} k_n \left(-\beta_n C_n + \beta_{n+2} C_{n+2}\right) = \frac{s C_6}{c}, \tag{49}$$

$$\sum_{n=1}^{2} k_n \left(-\beta_n C_n \mathrm{e}^{-k_n L} + \beta_{n+2} C_{n+2} \mathrm{e}^{k_n L}\right) = \frac{s C_6}{c} e^{-(s/\vartheta)L}. \tag{50}$$

Equations (47)–(50) form a linear system of four equations for the unknown parameters C_n ($n = 1, 2, 3, 4$). These parameters are determined by solving the system numerically or symbolically.

The Riemann sum approximation technique serves as an effective numerical approach for calculating the inverse Laplace transform, particularly when finding an analytical solution proves challenging or unfeasible. The inverse Laplace transform is represented by the Bromwich integral, which often requires numerical computation in practical applications. This method reformulates the inverse Laplace transform integral into a finite series across selected points within the complex plane. The Bromwich integral can be numerically approximated as follows [65, 66]:

$$f(x,t) \approx \mathrm{e}^{\Psi t}\frac{\Delta\omega}{\pi}Re\sum_{n=1}^{N}\overline{f}(x,\Psi + in\Delta\omega)\,\mathrm{e}^{in\Delta\omega t}. \tag{51}$$

In this context, Ψ is a real constant that guarantees that $\overline{f}(x,s)$ is analytic to the right of the line $Re(s) = \Psi$. Typically, Ψ is chosen as a small positive value. Additionally, $\Delta\omega$ represents the step size in the imaginary direction, while N denotes the number of terms in the summation, which serves as the truncation limit. Here, i is the imaginary unit defined as $i = \sqrt{-1}$.

5 Numerical results

This section presents a numerical case study focused on determining and examining the variations in temperature $\theta(x,t)$, displacement $u(x,t)$, and nonlocal thermal stress $\tau_{xx}(x,t)$ within a copper rod subjected to a mobile heat source. It also considers the implications of nonlocal elasticity and fractional heat conduction. The findings will demonstrate the interplay between these factors and their impact on the rod's behavior under the given circumstances. The numerical analysis utilizes the mechanical and thermoelastic properties of copper detailed below [67].

The material properties are characterized by a thermal conductivity of $K = 386\mathrm{W\ m^{-1}K^{-1}}$ and a specific heat of $C_E = 384.56$ J/kgK. The coefficient of thermal expansion is $\alpha_t = 1.78 \times 10^{-5}\ \mathrm{K^{-1}}$, while the density is $\rho = 8954\ \mathrm{Kgm^{-3}}$. The Lamé constant is given as $\lambda_e = 7.76 \times 10^{10}\ \mathrm{Nm^{-1}}$, and the shear modulus is $\mu_e = 3.86 \times 10^{10}\ \mathrm{Nm^{-1}}$. The reference temperature is set at $T_0 = 293$ K.

In terms of electrical properties, the electrical conductivity is $\sigma_0 = \frac{10^{-9}}{36\pi}Fm^{-1}$, and the magnetic permeability is $\mu_0 = \frac{4\pi}{10^7}Hm^{-1}$. The magnetic field strength is represented as $H_x = \frac{10^{-7}}{4\pi}\ \mathrm{Am^{-1}}$. The viscoelastic relaxation times are specified as $\lambda_0 = 0.05$ s and $\mu_0 = 0.1$ s. Finally, the delay times are noted as $\tau_\theta = 0.05$ s and $\tau_q = 0.1$ s.

The numerical results for the $\theta(x,t)$, $u(x,t)$, and $\tau_{xx}(x,t)$ are obtained using Mathematica software. This is achieved by employing the Riemann sum approximation method (51) to perform numerical computations of the inverse Laplace transforms. The field variables are evaluated over the domain $x \in [0, 10]$, allowing for a detailed analysis of the system's behavior within this range.

The findings are showcased visually in Figs. 2 to 10 and Tables 1–3, highlighting the influence of different factors on displacement, temperature, and nonlocal thermal stress. These graphical illustrations clearly depict how the system responds to various parametric conditions, providing a thorough insight into the fundamental dynamics at play. The

numerical outcomes uncover the cumulative effects of nonlocal elasticity in both spatial and temporal dimensions (ℓ and τ), fractional operators, the velocity of the moving heat source, and rotational movements on the thermoelastic response of the rod.

5.1 Effect of rotation parameter Ω on thermoelastic fields

Grasping the intertwined mechanical and thermal behaviors of a rotating rod necessitates an in-depth examination that takes into account the physical forces at play and the properties of the material itself. This evaluation is vital for the design and functionality of devices and structures where rotating rods play a crucial role, including turbines, aerospace technologies, and rotating shafts within machinery.

As a rod spins, the coupling between mechanical and thermal stresses is dictated by the rotation speed (Ω). The interaction between thermal expansion from heat and mechanical strain from rotation generates intricate stress distributions throughout the rod. This section explores how the rotation parameter Ω affects the thermoelastic fields of a rotating rod under the generalized heat conduction framework utilizing the tempered-Caputo fractional derivative (CT). The analysis presents results for rotation parameters set at $\Omega = 0, 1, 3$, and 5, while keeping other parameters constant ($\alpha = 0.75$, $\xi = 0.1$, $\vartheta = 2$, $\ell = 0.01$, and $\tau = 0.02$). The numerical outcomes are visually represented in Figs. 1, 2, and 3, illustrating the fluctuations in the thermoelastic fields along the rod's length within the range $x \in [0, 10]$.

The findings underscore the importance of accounting for rotational impacts when designing and analyzing rotating elements in engineering contexts, especially for high-speed machinery and nanomechanical systems. By integrating nonlocal elasticity and fractional heat conduction into the analysis, a more realistic and precise depiction of the physical behavior is achieved, enhancing the reliability and performance of such components.

Figure 2 depicts the correlation between temperature θ and the rotation parameter Ω. In Fig. 2, we see that at one end of the rod ($x = 0$), the temperature θ initially begins near zero, rapidly ascends due to the influence of a heat source, and then symmetrically declines to zero at the other end ($x = L$), adhering to the thermal boundary conditions that prevent heat from flowing out at the ends. The results indicate that the rotation parameter Ω has

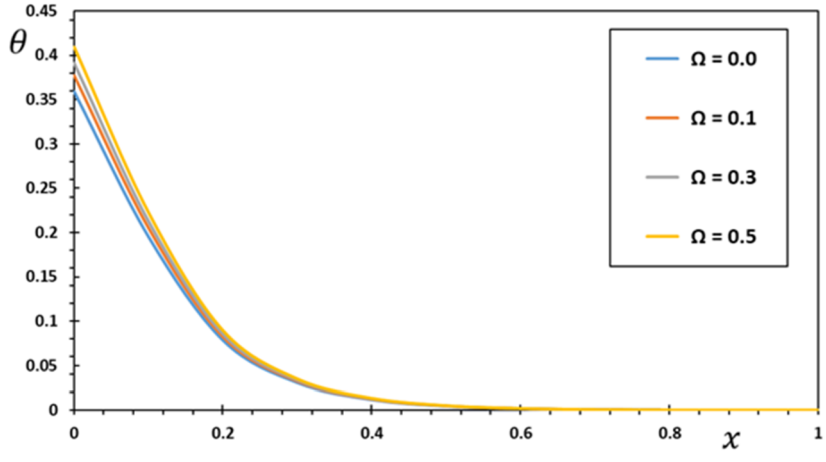

Figure 2 The temperature variation θ under the influence of angular velocity of rotation (Ω)

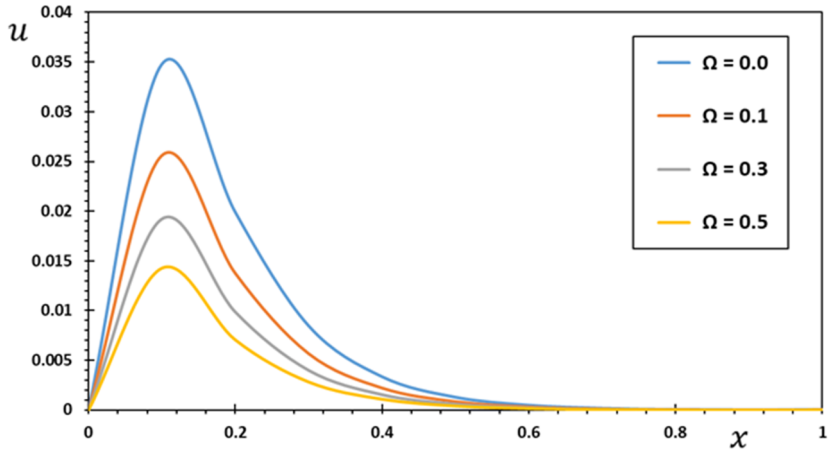

Figure 3 The displacement u under the influence of angular velocity of rotation (Ω)

a minimal impact on the temperature distribution θ. Additionally, as Ω increases, a slight decrease in temperature is observed due to the centrifugal force that alters the distribution of thermal energy within the rod. Overall, the temperature variation θ along the rod is largely driven by the heat source and the material's thermal properties, while the role of the rotation Ω is relatively minor, leading to only a subtle reduction in temperature with rising values of Ω.

Figure 3 demonstrates how displacement $u(x)$ varies with the rotation parameter Ω. The curves show that displacement starts at zero at one end of the rod, satisfying the fixed boundary condition. It dips to a minimum, then rises again, ultimately approaching zero near the free end, following the stress-free boundary condition. The rotation parameter Ω significantly influences the displacement profile; as the rotation parameter Ω increases, the displacement curves shift upward. This upward movement is attributed to greater centrifugal forces at higher rotation speeds, which stretch the rod and produce larger displacements. Displacement $u(x)$ is highly sensitive to alterations in Ω, with higher values resulting in more pronounced magnitudes of displacement due to the intensified centrifugal effects.

Figure 4 illustrates how nonlocal thermal stress $\tau_{xx}(x)$ varies with the rotation parameter Ω. It is evident that τ_{xx} starts at a minimum value at one end of the rod ($x = 0$) and rises to a peak around $x = 1$. Following this maximum, the stress then declines, nearing zero at the free end of the rod ($x = L$). The findings indicate that nonlocal thermal stress $\tau_{xx}(x)$ markedly increases as the rotation parameter Ω goes up. The centrifugal forces amplify the stress distribution, particularly in the central region of the rod ($x \approx 1$). While nonlocal effects contribute to a more uniform stress distribution, the influence of Ω significantly elevates the overall stress levels. The response of nonlocal thermal stress τ_{xx} to changes in Ω is pronounced; as rotation increases, so do the stress values, showcasing the combined effects of centrifugal forces and thermal expansion on the rod.

In the generalized model that includes rotation and fractional derivatives, the solutions are restricted to a finite spatial area, effectively illustrating a realistic speed of wave propagation. This model integrates the tempered-Caputo fractional derivative, which introduces memory effects that enhance the smoothness of both thermal and mechanical responses, making them more consistent with physical reality. In contrast, classical ther-

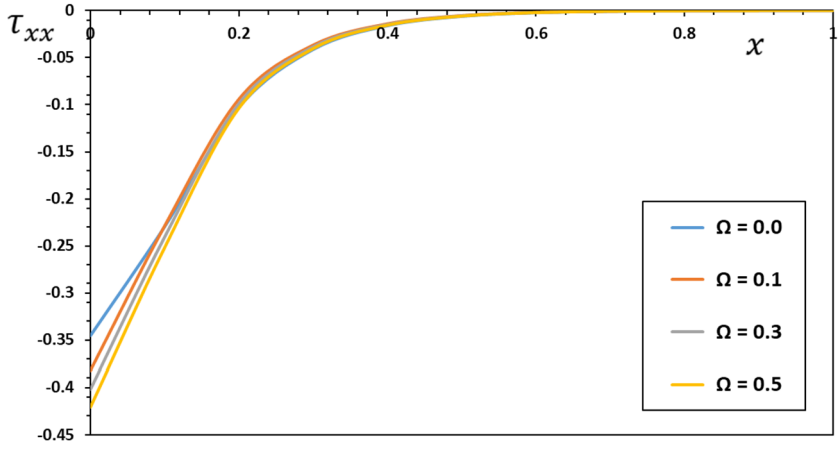

Figure 4 The nonlocal thermal stress τ_{xx} under the influence of angular velocity of rotation (Ω)

moelasticity suggests infinite wave propagation speeds, which are not physically realistic and do not match real-world observations. Furthermore, within the classical framework, solutions can diverge or exhibit unbounded behavior when faced with high rotation conditions, resulting in predictions that may lack reliability for practical applications.

The findings emphasize the significant impact of the rotation parameter ω on the thermoelastic properties exhibited by a rotating rod. It stresses the necessity of incorporating rotational effects into the design and analysis of engineering components that rotate, particularly in high-speed machinery and nanomechanical systems. By combining nonlocal elasticity with fractional heat conduction, the study achieves a more accurate and realistic representation of the physical behaviors at play.

5.2 Effect of fractional operators and fractional order parameter α

This subsection investigates how fractional operators and the fractional order α affect the thermoelastic response of conductive materials when subjected to an initial magnetic field. A comparative analysis is conducted among the tempered-Caputo fractional derivative (CT), the Caputo fractional derivative (C), and the classical scenario ($\alpha = 1$) within the framework of the generalized DPL theory of thermoelasticity. The results are numerically evaluated for fixed values of $\Omega = 3$, $\vartheta = 2$, $\ell = 0.01$, and $\tau = 0.02$, and graphically represented to highlight the effects of α on the fields.

In the classical case where $\alpha = 1$, the model follows the DPL approach of generalized thermoelasticity with one relaxation time, which leads to instantaneous wave propagation and aligns with classical theories of heat transport. In the fractional case where $0 < \alpha < 1$, the model uses the tempered-Caputo fractional derivative (CT) and Caputo fractional derivative (C) to alter the heat transport equation by adding fractional memory effects. This is specifically examined at $\alpha = 0.85$ and $\alpha = 0.75$, allowing for an analysis of how the fractional operator impacts thermal and mechanical wave behaviors.

As seen in Fig. 5, the thermodynamic temperature θ along the rod begins near zero at the first end ($x = 0$) where the heat source is applied, sharply rises to a maximum, and then symmetrically decreases to zero at the second end ($x = 0$), meeting the thermal boundary conditions of no heat flux at the ends. As the fractional order α rises from 0.5 to 1, there is a noticeable increase in temperature θ. In the classical LS model at $\alpha = 1$, the rate

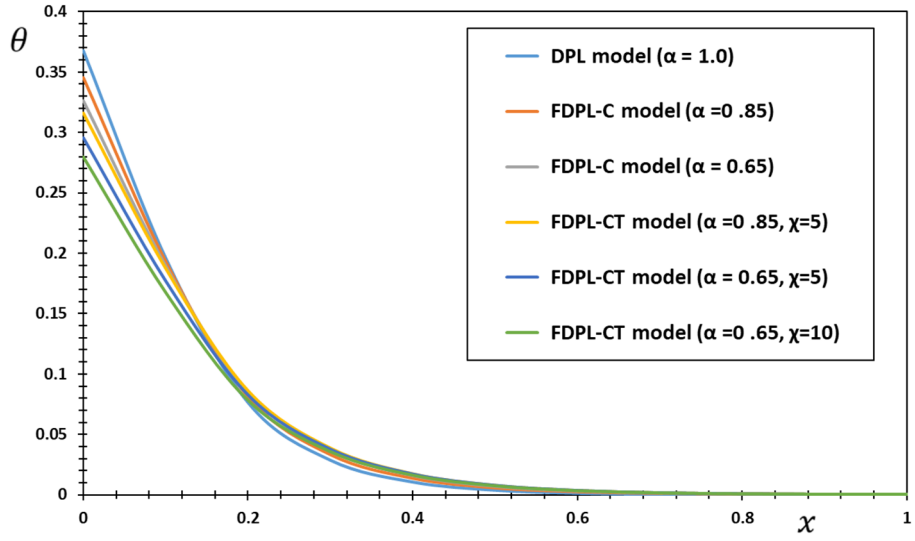

Figure 5 Temperature change θ for varying fractional operators and fractional order α

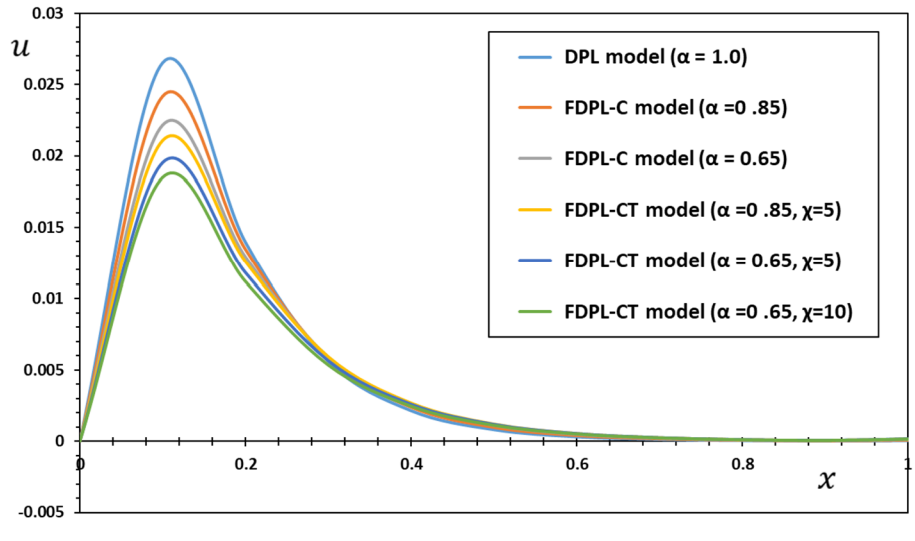

Figure 6 The displacement u for varying fractional operators and fractional order α

of temperature propagation is faster, reaching higher values compared to fractional scenarios (α = 0.85, 0.75). When lower values of α are used, incorporating memory effects through the tempered-Caputo derivative slows down the movement of the temperature wave, leading to lower peak temperatures and a more gradual decrease in temperature along the rod. A significant takeaway is that a higher fractional order α accelerates temperature wave propagation while increasing the thermodynamic temperature θ.

Figure 6 shows that the displacement magnitude u along the rod starts at zero at one end ($x = 0$), owing to the constant boundary condition, rises to a peak, and then tapers back to zero at the other end ($x = L$), where a stress-free boundary condition is in effect. From this, we can infer that increasing the fractional order α leads to a reduction in the propagation of the displacement u along the rod. Furthermore, within the classical DPL thermoelas-

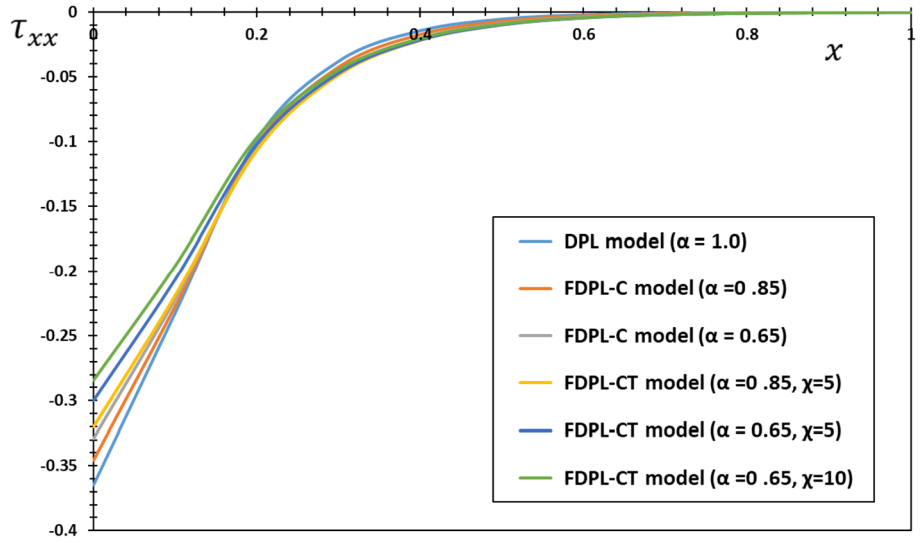

Figure 7 The nonlocal thermal stress τ_{xx} for varying fractional operators and fractional order α

tic model at $\alpha = 1$, the displacement achieves its maximum value without showing any memory effects. Conversely, for fractional values like $\alpha = 0.85$ and $\alpha = 0.75$, the tempered-Caputo factor introduces damping effects that reduce the displacement magnitudes and slow down the propagation of displacement waves. Hence, it is clear that lower fractional orders α contribute to a decrease in displacement u, as the fractional factors dampen wave amplitude by utilizing memory effects.

Figure 7 demonstrates that the nonlocal thermal stress τ_{xx} starts off with negative but nonzero values at one end, peaks near the heat source, and then gradually tapers to zero at the other end. This pattern illustrates the combined effects of thermal, mechanical, and nonlocal influences. A decrease in the fractional order α is linked to a reduction in the nonlocal stress τ_{xx}. At $\alpha = 1$, corresponding to the classical DPL thermoelastic model, stress levels peak due to the accelerated wave propagation. In contrast, for the fractional values $\alpha = 0.85$ and $\alpha = 0.75$, the introduction of the fractional operator results in damping effects that reduce stress magnitudes and slow down the stress wave's propagation. Therefore, it can be concluded that higher fractional orders α lead to increased nonlocal thermal stress τ_{xx}, largely due to the damping effects of fractional memory on the propagation of stress.

The findings emphasize the crucial function of fractional operators, especially the tempered-Caputo derivative, in simulating the behavior of nonlocal thermoelastic materials. The fractional order α serves as an adjustable parameter that controls wave propagation, memory effects, and field distributions, making it an invaluable asset for investigating advanced materials. These results showcase the adaptability of the generalized thermoelastic model with tempered-Caputo fractional derivatives in accurately reflecting realistic material behaviors. Fractional models play a key role in thermal management, enabling the design of materials with tailored thermal propagation characteristics, particularly beneficial for electronics and aerospace sectors. The tempered-Caputo framework is particularly advantageous in the realm of nanomechanics, where nonlocal and memory effects are commonly observed in materials at the nanoscale. Additionally, the impact of α can be harnessed in material design to engineer materials with specific mechanical or

thermal responses, which is especially valuable for applications like shock absorbers or heat sinks.

5.3 The effect of moving heat source velocity parameter

When investigating the impact of altering the velocity parameter ϑ of a moving heat source, denoted as $Q = Q_0\delta(x - \vartheta t)$, on key physical properties like temperature, displacement, nonlocal thermal stress, and strain, it is essential to grasp how these changes shape the material's behavior. The velocity of the heat source modifies nonlocal interactions by affecting the rate at which the thermal field fluctuates in both space and time. A quicker movement of the heat source tends to amplify nonlocal effects over a larger area, potentially resulting in lower peak stress even as the zone of influence expands. This dynamic creates a complex interplay that significantly alters the material's response to thermal stimuli.

This subsection delves into how the velocity of the heat source ϑ affects the thermal and mechanical behavior of nanorods, a critical aspect in the design and assessment of nanosystems exposed to dynamic thermal loads. Figures 8 to 10 present a comprehensive analysis of these variations, emphasizing the complex interplay between heat source velocity and the resulting characteristics of the material's response.

From Fig. 8, it is evident that as the velocity of the heat source (ϑ) increases, the peak temperature θ along the rod decreases. This decrease occurs because each point along the rod is exposed to heat for a shorter duration. Consequently, several outcomes arise: there are lower peak temperatures θ, a more rapid decay of temperature (θ) along the rod's length, and a reduction in the amplitude of temperature oscillations. These effects underscore the essential impact of heat source velocity (ϑ) in determining the thermal dynamics of the system.

As shown in Fig. 9, higher heat source velocities result in greater displacements u at various locations along the rod. This occurs due to two main reasons: the generation of steeper thermal gradients from the swiftly moving sources, and the increased thermal distortion resulting from these gradients. This connection emphasizes the pivotal role of velocity in influencing the rod's mechanical response.

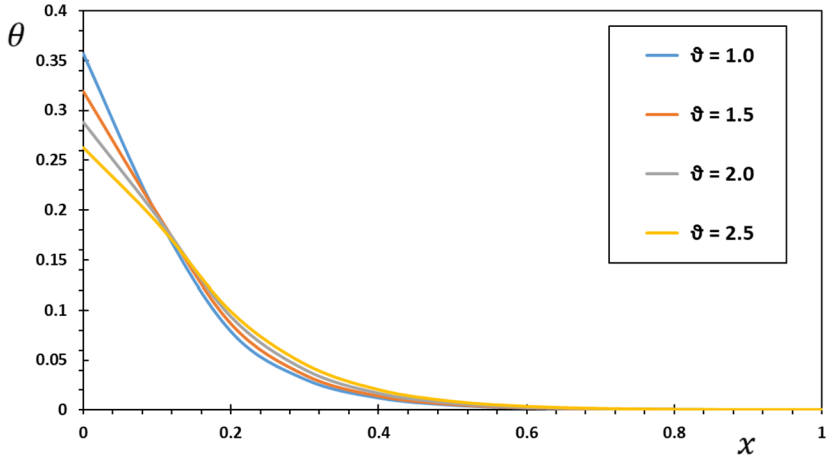

Figure 8 Effect of varying heat source velocity ϑ on temperature θ

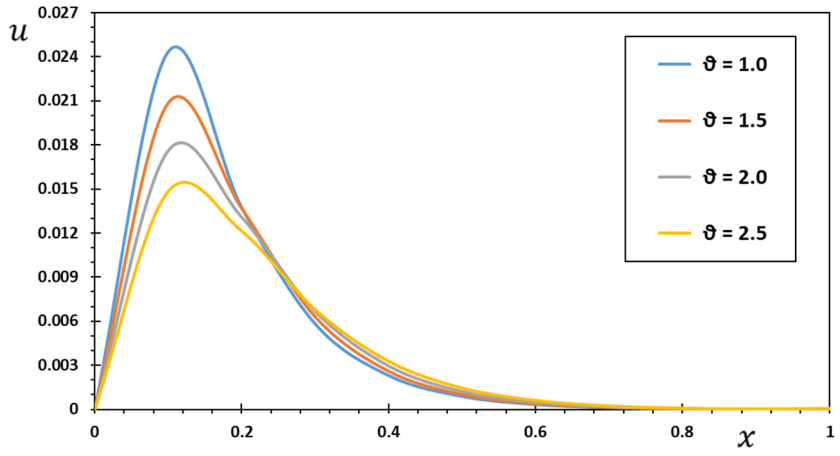

Figure 9 Effect of varying heat source velocity ϑ on displacement u

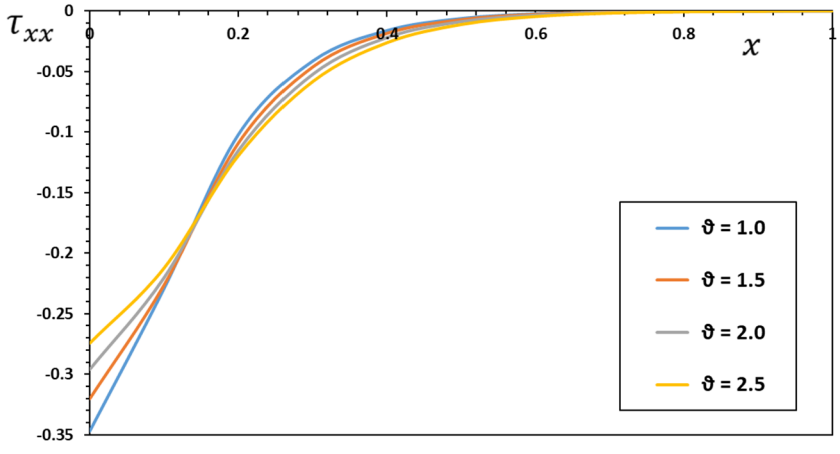

Figure 10 Effect of varying heat source velocity ϑ on nonlocal thermal stress τ_{xx}

Figure 10 indicates that as the heat source velocity increases, the total nonlocal thermal stress τ_{xx} also rises. This rise can be linked to two fundamental reasons: the formation of more pronounced temperature gradients due to the increased velocities and the heightened thermal stresses that arise from these sharp gradients. This relationship highlights the crucial influence of heat source velocity on the thermal stress experienced by the rod.

The numerical results and analysis demonstrate that the motion velocity coefficient ϑ of the heat source significantly influences the behavior of various physical fields, including temperature θ, displacement u, and thermal stress τ_{xx}. The results reveal that with an increase in ϑ, there is a corresponding enhancement in thermal gradients, which leads to greater displacement, stress, and strain experienced along the rod. Interestingly, while these factors rise, the temperature θ tends to decrease as ϑ ascends, mainly because there is less time for local heat to accumulate. Furthermore, the moving heat source creates concentrated thermal and mechanical effects, especially near its path, resulting in notable spikes in displacement, stress, and strain. However, these peaks tend to fade as one moves further from the heat source, a finding that is consistent with existing research. Further-

more, heat sources that move at higher speeds enable a more rapid spread of thermal and mechanical responses along the rod. As the velocity c of the heat source increases, the oscillatory patterns in these fields become less pronounced. This decline in oscillations happens because the swift movement of the heat source restricts the formation of significant fluctuations.

The noted decrease in temperature with an increase in heat source velocity demonstrates how the motion of the heat source affects the rate of heat diffusion. Swiftly moving heat sources produce weaker thermal fields, which can be advantageous in preventing overheating in nanoscale devices. On the other hand, the rise in displacement, stress, and strain that accompanies an increase in ϑ emphasizes the importance of factoring in thermal deformation when designing nanorods exposed to dynamic heating. If not carefully controlled, these rapid heat sources can create high mechanical stresses, risking material failure. This research offers critical insights into the behavior of nanorods under dynamic thermal conditions. The findings lay groundwork for improving various applications: thermal actuators where managed displacement is vital, nanosensors that depend on accurate stress or strain measurements, and heat conduction systems that effectively address thermal gradients.

5.4 The effect nonlocal length and time scale parameters

The incorporation of the Klein–Gordon operator in the theoretical analysis provides a more detailed representation of the dynamics within elastic materials, especially at the nanoscale. By including nonlocal length scale ℓ and time scale τ parameters, this approach effectively captures size-dependent behaviors and memory effects that traditional local elasticity theories often miss. These enhancements are crucial for understanding nanostructured materials as their mechanical and thermal performance is significantly influenced by spatial and temporal interactions.

The importance of nonlocal parameters in modeling nanostructures is highlighted through the inclusion of nonlocal length scale (ℓ) and time scale (τ) factors. The length scale ℓ captures spatial nonlocality, indicating that the stress or strain at a given point is affected by the stress or strain in nearby locations. This aspect is essential for introducing size effects, allowing the model to forecast behaviors that are sensitive to the nanostructure's dimensions, such as a decrease in stiffness or wave dispersion. At the nanoscale, ℓ becomes particularly vital as it accounts for the impact of atomic-scale interactions and long-range forces, which play a significant role at this scale. The parameter τ signifies temporal nonlocality, integrating memory effects into the model. This is crucial for reflecting the material's capability to "recall" previous states, thereby affecting its present response. Memory effects are especially pertinent in viscoelastic or thermoelastic systems, where the response of the material is heavily influenced by time-dependent relaxation processes and thermal histories.

The Klein–Gordon operator, expressed as $\left(1 - \ell^2\nabla^2 + \tau^2\frac{\partial^2}{\partial t^2}\right)$, integrates both spatial and temporal nonlocality. It facilitates the modeling of phenomena such as wave dispersion, finite propagation speeds, and the interaction between spatial and temporal scales. This operator is vital for effectively modeling wave dynamics in nanostructures, offering a more accurate representation compared to classical elasticity theories, which frequently suggest infinite wave speeds or fail to consider size-dependent effects.

When assessing the behavior of a nanobeam under both local and nonlocal conditions, the differences between these models are defined by the presence or absence of nonlocal

parameters ℓ and τ. The local thermoelastic model, which assumes $\ell = 0$ and $\tau = 0$, claims that the stress at any location is solely linked to the strain at that same point. It overlooks memory effects and ignores the influence of neighboring points. As a result, this model often overestimates thermal gradients, leading to an accelerated heat transfer and unrealistically infinite thermal wave speeds, while demonstrating mechanical behavior that does not vary with size. In contrast, the nonlocal thermoelastic model, which takes various combinations of ℓ and τ into account, reveals notable discrepancies in its predictions.

The spatial nonlocality parameter ℓ considers the effects of strains and stresses from nearby points, leading to a reduction in the overall magnitude of stress and strain, smoothing out variations, and introducing size-dependent behaviors. This modification enables a more precise portrayal of physical behaviors in nanostructures, where atomic-scale interactions hold considerable importance. On the other hand, the temporal nonlocality parameter τ allows the model to account for damping and delays in wave propagation, showcasing the material's capacity to retain memory and gradually adjust to changes over time. This aspect is particularly significant in viscoelastic or thermoelastic materials, where relaxation and memory effects play a crucial role in determining their response. The findings presented in Tables 1, 2, and 3 illustrate how the parameters ℓ and τ influence the behavior of a nanobeam when examined through both local and nonlocal models.

The local model suggests unrealistic infinite thermal wave speeds. Conversely, the nonlocal model guarantees finite speeds with the influence of τ and promotes a more even heat distribution as ℓ increases, leading to decreased thermal gradients. While the local model, assuming $\ell = 0$ and $\tau = 0$, inaccurately states that displacement is unaffected by

Table 1 Influence of the spatial and temporal nonlocality on the temperature θ

	$\ell = 0.000$, $\tau = 0.000$	$\ell = 0.001$, $\tau = 0.000$	$\ell = 0.000$, $\tau = 0.002$	$\ell = 0.003$, $\tau = 0.002$	$\ell = 0.005$, $\tau = 0.002$	$\ell = 0.003$, $\tau = 0.004$
0	0.357215	0.342936	0.332219	0.321502	0.310786	0.296497
0.1	0.194764	0.18698	0.181137	0.175294	0.169451	0.16166
0.2	0.0786352	0.0754926	0.0731335	0.0707744	0.0684152	0.0652697
0.3	0.0307695	0.0295389	0.0286158	0.0276928	0.0267697	0.0255389
0.4	0.0119938	0.011513	0.0111532	0.0107934	0.0104336	0.00995392
0.5	0.00467362	0.00448526	0.0043451	0.00420493	0.00406477	0.00387788
0.6	0.00182217	0.00174794	0.00169332	0.00163869	0.00158407	0.00151124
0.7	0.000712475	0.000682889	0.000661549	0.000640209	0.000618869	0.000590415
0.8	0.000283295	0.000271182	0.000262707	0.000254233	0.000245758	0.000234459
0.9	0.000124412	0.000118923	0.000115206	0.00011149	0.000107774	0.000102819
1.0	8.41936E-05	8.04411E-05	7.79274E-05	7.54136E-05	7.28998E-05	6.95481E-05

Table 2 Influence of the spatial and temporal nonlocality on the displacement u

	$\ell = 0.000$, $\tau = 0.000$	$\ell = 0.001$, $\tau = 0.000$	$\ell = 0.000$, $\tau = 0.002$	$\ell = 0.003$, $\tau = 0.002$	$\ell = 0.005$, $\tau = 0.002$	$\ell = 0.003$, $\tau = 0.004$
0	0	0	0	0	0	0
0.1	0.0260673	0.0243436	0.021293	0.0188034	0.0157623	0.0136873
0.2	0.0136836	0.0137868	0.0136393	0.013212	0.0123126	0.0114557
0.3	0.0056229	0.00586163	0.00626896	0.00654388	0.00673533	0.00672781
0.4	0.00221204	0.00233347	0.00260135	0.00286545	0.00321482	0.00344004
0.5	0.000863532	0.000914157	0.00103958	0.00118728	0.00143177	0.0016356
0.6	0.000336549	0.000356628	0.00040924	0.000478406	0.000612243	0.000743966
0.7	0.000130817	0.000138682	0.000159879	0.000189812	0.000255268	0.000329132
0.8	5.01285E-05	0.000053334	6.21108E-05	0.000074969	0.00010578	0.000144985
0.9	1.94408E-05	2.17027E-05	2.66512E-05	3.30645E-05	4.87466E-05	7.07818E-05
1.0	4.89405E-05	4.22984E-05	3.69413E-05	3.66782E-05	4.37747E-05	5.84547E-05

Table 3 Influence of the spatial and temporal nonlocality on the nonlocal thermal stress τ_{xx}

	$\ell = 0.000$, $\tau = 0.000$	$\ell = 0.001$, $\tau = 0.000$	$\ell = 0.000$, $\tau = 0.002$	$\ell = 0.003$, $\tau = 0.002$	$\ell = 0.005$, $\tau = 0.002$	$\ell = 0.003$, $\tau = 0.004$
0	–0.361024	–0.347027	–0.305166	–0.281201	–0.263667	–0.249645
0.1	–0.229759	–0.229417	–0.221993	–0.213907	–0.206475	–0.199703
0.2	–0.0988773	–0.10243	–0.113164	–0.117984	–0.120411	–0.121552
0.3	–0.0392567	–0.0413137	–0.0502265	–0.0566151	–0.0614414	–0.0651878
0.4	–0.0153513	–0.0162396	–0.0209512	–0.025294	–0.029181	–0.0326258
0.5	–0.00598763	–0.00634363	–0.00847448	–0.0108378	–0.0132598	–0.0156389
0.6	–0.00233531	–0.0024752	–0.00337346	–0.00452191	–0.00584731	–0.00727556
0.7	–0.000913016	–0.000967783	–0.00133291	–0.00185311	–0.00252017	–0.003303
0.8	–0.000362506	–0.000383713	–0.00052614	–0.000746207	–0.00105561	–0.00144735
0.9	–0.000153574	–0.000158566	–0.000199794	–0.000275389	–0.000392345	–0.000550437
1.0	0	0	0	0	0	0

size, the nonlocal model shows that as ℓ increases, displacement decreases due to strain redistribution. Additionally, higher τ values enhance this effect through damping. Under the local model, stress tends to be overestimated, especially near edges or load application points. In contrast, the nonlocal model moderates stress with a greater ℓ, effectively smoothing out the stress distribution, and introduces a delay in stress response with rising τ, simulating time-dependent relaxation.

The numerical findings indicate that incorporating the parameters ℓ and τ into the Klein–Gordon operator significantly deepens our comprehension and forecasting of material behavior at the nanoscale, which carries profound implications across several applications. These insights are particularly valuable for mechanical devices operating on a small scale, as they allow for precise predictions of stress and strain distribution in structures like beams, rods, and plates. Such accuracy is essential for the effective design of actuators and mechanical resonators. Moreover, the results contribute to improved thermal management in nanosystems by shedding light on how nonlocal thermal conduction affects temperature distribution. This knowledge is crucial for the development of sensors, heat sinks, and heat engines designed at the nanoscale. The size-dependent behaviors encapsulated by these parameters ultimately enhance the design of material properties in nanocomposites and metamaterials, driving progress in materials engineering. Ultimately, the results highlight the limitations of traditional local models when analyzing nanostructured materials, underscoring the critical role of nonlocal theories in the fields of nanotechnology and materials science.

Some similar results can be found in [68–70].

6 Conclusions

The study addresses the complex dynamics of a rotating nanorod subjected to a moving heat source, using two sophisticated theoretical frameworks: the Klein–Gordon type nonlocal theory and a fractional heat conduction model. This innovative approach aims to capture the nuanced behavior of nanoscale structures under thermal and mechanical influences, a topic of significant interest for advanced material engineering and nanotechnology applications. The theoretical model achieves its sophistication through the seamless integration of multiple advanced concepts: nonlocal elasticity, fractional heat conduction, Kelvin–Voigt viscoelasticity, and magnetic forces. This unified approach creates a robust platform for analyzing complex nanoscale system behaviors. The numerical simulations powerfully demonstrate that accurate predictions of thermal and mechanical

responses require the incorporation of three key elements: fractional-order heat conduction, nonlocal effects, and viscoelastic damping. These findings establish a new standard for modeling nanoscale systems, offering enhanced precision and reliability in predicting material behavior.

Based on the detailed discussions and analysis of the parameters influencing the thermoelastic behavior of rotating viscoelastic nanorods subjected to moving heat sources, the following key conclusions can be drawn:

- The integration of the Klein–Gordon operator into the governing equations effectively captures essential nonlocal spatial and temporal effects that are significant at the nanoscale. The inclusion of nonlocal length scale and time scale parameters enables a precise representation of size-dependent behaviors, such as stiffness reduction and stress redistribution in nanorods, as well as the memory effects influencing wave propagation and relaxation in viscoelastic materials.
- The use of the tempered-Caputo fractional derivative introduces critical nonlocality and memory effects into the heat conduction model, ensuring finite thermal wave speeds. The fractional and tempering parameters control thermal dissipation and the velocity of thermal wave propagation, resulting in physically realistic thermal responses. This fractional approach offers superior accuracy over classical heat conduction models in predicting temperature distributions in nanorods and better captures the localized heat effects of moving heat sources.
- The Kelvin–Voigt viscoelastic framework successfully accounts for damping effects and energy dissipation in materials subjected to dynamic loads. This viscoelasticity plays a significant role in shaping the mechanical response, reducing displacement and strain amplitudes through relaxation effects and creating smoother stress distributions across the material.
- Rotation proves to be a critical factor affecting all thermoelastic fields, increasing displacement through centrifugal forces and amplifying thermal stress and strain. The interaction between rotation and nonlocality results in complex dynamics that necessitate advanced modeling techniques. Additionally, the velocity of moving heat sources has a notable impact on both thermal and mechanical fields, with higher velocities leading to lower temperatures but higher displacement, thermal stress, and strain.
- These findings provide crucial insights for advancing nanoengineering technologies, contributing to the optimization of nanoscale devices operating in dynamic and complex environments.

Acknowledgements
The authors present their appreciation to King Saud University for funding the publication of this research through the Researchers Supporting Program (RSPD2025R1003), King Saud University, Riyadh, Saudi Arabia.

Author contributions
A.E.A. and S.S.A. wrote the main manuscript text, and A.F. prepared the figures and M.M. supervised the math relations. All authors reviewed the manuscript.

Funding
This project is funded by King Saud University, Riyadh, Saudi Arabia.

Data availability
No datasets were generated or analysed during the current study.

Declarations

Competing interests
The authors declare no competing interests.

Author details
[1]Department of Mathematics, Faculty of Science, Mansoura University, Mansoura 35516, Egypt. [2]Department of Mathematics and Computer Science, Transilvania University of Brasov, Brasov, Romania. [3]Academy of Romanian Scientists, Ilfov Street, 3, 050045 Bucharest, Romania. [4]Department of Statistics and Operations Research, College of Science, King Saud University, P.O. Box 2455, Riyadh 11451, Saudi Arabia.

Received: 5 December 2024 Accepted: 1 January 2025 Published online: 20 January 2025

References

1. Lakes, R.S.: Viscoelastic Materials. Cambridge University Press, Cambridge (2009)
2. Knauss, W.G.: A review of fracture in viscoelastic materials. Int. J. Fract. **196**, 99–146 (2015)
3. Koruk, H., Rajagopal, S.: A comprehensive review on the viscoelastic parameters used for engineering materials, including soft materials, and the relationships between different damping parameters. Sensors **24**(18), 6137 (2024)
4. Yazdanparast, R., Rafiee, R.: A 3D nonlinear viscoelastic–viscoplastic constitutive model for dynamic response of an epoxy resin. Acta Mech. **235**(11), 6625–6639 (2024)
5. Su, X., Yao, D., Xu, W.: A new method for formulating linear viscoelastic models. Int. J. Eng. Sci. **156**, 103375 (2020)
6. Li, X., Sha, A., Song, R., Jiao, W.: Fractional viscoelastic constitutive modelling of real-time strain response for asphalt pavement composites subjected to simulating wheel loadings. Int. J. Pavement Eng. **25**(1), 2380526 (2024)
7. Zheng, G., Zhang, N., Lv, S.: The application of fractional derivative viscoelastic models in the finite element method: taking several common models as examples. Fractal Fract. **8**(2), 103 (2024)
8. Hilfer, R. (ed.): Applications of Fractional Calculus in Physics World Scientific, Singapore (2000)
9. Das, S.: Functional Fractional Calculus, vol. 1. Springer, Berlin (2011)
10. Shams, M., Kausar, N., Samaniego, C., Agarwal, P., Ahmed, S.F., Momani, S.: On efficient fractional Caputo-type simultaneous scheme for finding all roots of polynomial equations with biomedical engineering applications. Fractals **31**(04), 2340075 (2023)
11. Alfadil, H., Abouelregal, A.E., Civalek, Ö., Öztop, H.F.: Effect of the photothermal Moore–Gibson–Thomson model on a rotating viscoelastic continuum body with a cylindrical hole due to the fractional Kelvin-Voigt model. Indian J. Phys. **97**(3), 829–843 (2023)
12. Elsamani, S.A., Mohmmed, A.A., Kogan, K.M., Salih, S.Y.M., Ahmed, I.A.: Fractional calculus applications in engineering insights into four-dimensional chaotic systems. J. Theory Math. Phys. **3**(5), 75–84 (2024)
13. Ferrari, A.L., Gomes, M.C.S., Aranha, A.C.R., Paschoal, S.M., de Souza Matias, G., de Matos Jorge, L.M., Defendi, R.O.: Mathematical modeling by fractional calculus applied to separation processes. Sep. Purif. Technol. **337**, 126310 (2024)
14. Ganie, A.H., Mofarreh, F., Khan, A.: A fractional analysis of Zakharov–Kuznetsov equations with the Liouville–Caputo operator. Axioms **12**(6), 609 (2023)
15. Korichi, Z., Souigat, A., Bekhouche, R., Meftah, M.T.: Solution of the fractional Liouville equation by using Riemann–Liouville and Caputo derivatives in statistical mechanics. Theor. Math. Phys. **218**(2), 336–345 (2024)
16. Caputo, M., Fabrizio, M.: A new definition of fractional derivative without singular kernel. Prog. Fract. Differ. Appl. **1**(2), 73–85 (2015)
17. Caputo, M., Fabrizio, M.: On the notion of fractional derivative and applications to the hysteresis phenomena. Meccanica **52**, 3043–3052 (2017)
18. Atangana, A., Baleanu, D.: New fractional derivatives with nonlocal and non-singular kernel: theory and application to heat transfer model. Therm. Sci. **20**, 763–769 (2016)
19. Gomez-Aguilar, J.F., Atangana, A. (eds.): Applications of Fractional Calculus to Modeling in Dynamics and Chaos CRC Press, Boca Raton (2022)
20. Mainardi, F.: Why the Mittag-Leffler function can be considered the queen function of the fractional calculus? Entropy **22**(12), 1359 (2020)
21. Atanackovic, T.M.: Stability Theory of Elastic Rods, vol. 1. World Scientific, Singapore (1997)
22. Mikhasev, G., Avdeichik, E., Prikazchikov, D.: Free vibrations of nonlocally elastic rods. Math. Mech. Solids **24**(5), 1279–1293 (2019)
23. Khosravifard, A., Hematiyan, M.R., Ghiasi, N.: A meshfree method with dynamic node reconfiguration for analysis of thermo-elastic problems with moving concentrated heat sources. Appl. Math. Model. **79**, 624–638 (2020)
24. Abouelregal, A.E., Marin, M., Foul, A., Askar, S.S.: Thermomagnetic responses of a thermoelastic medium containing a spherical hole exposed to a timed laser pulse heat source. Case Stud. Therm. Eng. **56**, 104288 (2024)
25. Guo, Y., Xiong, C., Yu, W., Li, J., Ma, J., Du, C.: Coupling dynamic response of saturated soil with anisotropic thermal conductivity under fractional order thermoelastic theory. PLoS ONE **19**(4), e0297651 (2024)
26. Pham, C.V., Vu, T.N.A.: On the well-posedness of Eringen's non-local elasticity for harmonic plane wave problems. Proc. R. Soc. A **480**(2293), 20230814 (2024)
27. Arpanahi, R.A., Hashemi, K.H., Mohammadi, B., Hashemi, S.H.: Investigation of the vibration behavior of nano piezoelectric rod using surface effects and non-local elasticity theory. Eng. Res. Express **5**(3), 035029 (2023)
28. Eringen, A.C.: Nonlocal polar elastic continua. Int. J. Eng. Sci. **10**(1), 1–16 (1972)
29. Eringen, A.C., Edelen, D.: On nonlocal elasticity. Int. J. Eng. Sci. **10**(3), 233–248 (1972)
30. Eringen, A.C.: On differential equations of nonlocal elasticity and solutions of screw dislocation and surface waves. J. Appl. Phys. **54**(9), 4703–4710 (1983)
31. Wang, T., Zhang, X., He, T.: Investigation on thermoelastic wave propagation in viscoelastic single-walled carbon nanotubes with surface effect based on nonlocal elasticity and GN theory. Physica E, Low-Dimens. Syst. Nanostruct. **163**, 116038 (2024)
32. Singh, B.: Wave propagation in context of Moore–Gibson–Thompson thermoelasticity with Klein–Gordon nonlocality. Vietnam J. Mech. **46**(2), 104–118 (2024)

33. Islam, R., Kawser, M.A., Rana, M.S., Islam, M.N.: Mathematical analysis of soliton solutions in space-time fractional Klein-Gordon model with generalized exponential rational function method. Partial Differ. Equ. Appl. Math. **12**, 100942 (2024)
34. Odibat, Z.: Numerical simulation for an initial-boundary value problem of time-fractional Klein-Gordon equations. Appl. Numer. Math. **206**, 1–11 (2024)
35. Agiasofitou, E., Lazar, M.: Nonlocal elasticity of Klein–Gordon type with internal length and time scales: constitutive modelling and dispersion relations. PAMM **23**(3), e202300065 (2023)
36. Lazar, M., Agiasofitou, E., Po, G.: Three-dimensional nonlocal anisotropic elasticity: a generalized continuum theory of Ångström-mechanics. Acta Mech. **231**(2), 743–781 (2020)
37. Carrião, P.C., Lehrer, R., Vicente, A.: Unstable ground state and blow up result of nonlocal Klein–Gordon equations. J. Dyn. Differ. Equ. **35**(3), 1917–1945 (2023)
38. Lazar, M., Agiasofitou, E.: Nonlocal elasticity of Klein–Gordon type: fundamentals and wave propagation. Wave Motion **114**, 103038 (2022)
39. Zhmakin, A.I.: Heat conduction beyond the Fourier law. Tech. Phys. **66**, 1–22 (2021)
40. Lord, H.W., Shulman, Y.: A generalized dynamical theory of thermoelasticity. J. Mech. Phys. Solids **15**(5), 299–309 (1967)
41. Tzou, D.Y.: A unified approach for heat conduction from macro-to micro-scales. J. Heat Transf. **117**, 8–16 (1995)
42. Tzou, D.Y.: Macro- to Micro-Scale Heat Transfer: The Lagging Behavior. Taylor & Francis, Abingdon (1997)
43. Tzou, D.Y.: Experimental support for the lagging behavior in heat propagation. J. Thermophys. Heat Transf. **9**(4), 686–693 (1995)
44. Tzou, D.Y.: The generalized lagging response in small-scale and high-rate heating. Int. J. Heat Mass Transf. **38**(17), 3231–3240 (1995)
45. Guo, H., Xu, Z., Shang, F., He, T.: A new constitutive theory of nonlocal piezoelectric thermoelasticity based on nonlocal single-phase lag heat conduction and structural transient thermo-electromechanical response of piezoelectric nanorod. Mech. Adv. Mat. Struct. **31**(29), 11737–11754 (2024)
46. Guo, H., Shang, F., He, T.: Fractional-order rate-dependent piezoelectric thermoelasticity theory based on new fractional derivatives and its application in structural transient response analysis of smart piezoelectric composite laminates. Int. J. Appl. Mech. **16**(2), 2450016 (2024)
47. Li, C., Liu, J., He, T.: Fractional-order rate-dependent thermoelastic diffusion theory based on new definitions of fractional derivatives with non-singular kernels and the associated structural transient dynamic responses analysis of sandwich-like composite laminates. Commun. Nonlinear Sci. Numer. Simul. **132**, 107896 (2024)
48. Li, C., Guo, H., Tian, X., He, T.: Size-dependent thermo-electromechanical responses analysis of multi-layered piezoelectric nanoplates for vibration control. Compos. Struct. **225**, 111112 (2019)
49. Li, C., Lu, Y., Guo, H., He, T., Tian, X.: Non-Fick diffusion–elasticity based on a new nonlocal dual-phase-lag diffusion model and its application in structural transient dynamic responses. Acta Mech. **234**(7), 2745–2761 (2023)
50. Zhang, J., Ma, Y.: Investigation of the thermoelastic behaviour of magneto-thermo-viscoelastic rods based on the Kelvin-Voigt viscoelastic model. Iran. J. Sci. Technol. Trans. Mech. Eng. **48**, 1533–1549 (2023)
51. Abouelregal, A.E.: Thermo-viscoelastic properties in a non-simple three-dimensional material based on fractional derivative Kelvin–Voigt model. Indian J. Phys. **96**(2), 399–410 (2022)
52. Saada, A.S.: Elasticity: Theory and Applications, vol. 16. Elsevier, Amsterdam (2013)
53. Hetnarski, R.B., Ignaczak, J.: Generalized thermoelasticity. J. Therm. Stresses **22**(4–5), 451–476 (1999)
54. Al-Mazmumy, M., Alyami, M.A., Alsulami, M., Alsulami, A.S.: Reliable computational method for systems of fractional differential equations endowed with Ψ-Caputo fractional derivative. Contemp. Math. **5**(4), 4991–5011 (2024)
55. Medved', M., Pospíšil, M., Brestovanská, E.: A new nonlinear integral inequality with a tempered ψ-Hilfer fractional integral and its application to a class of tempered Ψ-Caputo fractional differential equations. Axioms **13**(5), 301 (2024)
56. Pospíšil, M., Brestovanská, E.: A new nonlinear integral inequality with a tempered Ψ-Hilfer fractional integral and its application to a class of tempered Ψ-Caputo fractional differential equations. Axioms **13**(5), 301 (2024)
57. Huang, J., Shao, L., Liu, J.: Well-posedness and an Euler–Maruyama method for multi-term Caputo tempered fractional stochastic differential equations. Phys. Scr. **99**(2), 025236 (2024)
58. Peng, W., Pan, B.: Fractional dual-phase-lag thermal-mechanical response of an functionally graded spherical microshell with size-dependent effect. J. Strain Anal. Eng. Des. **59**(3), 167–177 (2024)
59. Abouelregal, A.E., Alhassan, Y., Althagafi, H., Alsharif, F.: A two-temperature fractional DPL thermoelasticity model with an exponential Rabotnov kernel for a flexible cylinder with changeable properties. Fractal Fract. **8**(4), 182 (2024)
60. Abouelregal, A.E., Marin, M., Foul, A., Askar, S.S.: Thermomagnetic responses of a thermoelastic medium containing a spherical hole exposed to a timed laser pulse heat source. Case Stud. Therm. Eng. **56**, 104288 (2024)
61. Boora, K., Deswal, S., Kadian, A.: Thermo-mechanical interactions in a functionally graded orthotropic thermoelastic medium with rotation and gravity. Mech. Based Des. Struct. Mach. **52**(7), 4312–4336 (2024)
62. Othman, M.I., Said, S.M., Gamal, E.M.: Eigenvalue approach on a fiber-reinforced magneto-visco-thermoelastic rotating medium with initial stress. J. Vib. Eng. Technol. **12**(3), 5173–5187 (2024)
63. Abouelregal, A.E., Marin, M., Askar, S.S., Foul, A.: Transient thermoelastic response in a semi-infinite medium subjected to a moving heat source: an implementation of the Moore–Gibson–Thompson model with higher-order memory-dependent derivatives. Mech. Time-Depend. Mater. **28**, 1555–1581 (2024)
64. Abbas, I.A., Abdalla, A.N., Abbas, A.A.: The effect of a moving heat source and relaxation times on viscoelastic biological tissues during thermal treatments. Sohag J. Sci. **9**(4), 490–496 (2024)
65. Wilcox, D.J., Gibson, I.S.: Numerical Laplace transformation and inversion in the analysis of physical systems. Int. J. Numer. Methods Eng. **20**(8), 1507–1519 (1984)
66. Kitahara, N., Nagahara, D., Yano, H.: A numerical inversion of Laplace transform and its application. J. Franklin Inst. **325**(2), 221–233 (1988)
67. Singh, R.V., Mukhopadhyay, S.: Relaxation effects on thermoelastic interactions for time-dependent moving heat source under a recent model of thermoelasticity. Z. Angew. Math. Phys. **72**, 1–13 (2021)
68. Vlase, S., et al.: Coupled transverse and torsional vibrations in a mechanical system with two identical beams. AIP Adv. **7**(6), 065301 (2017)

69. Codarcea-Munteanu, L., et al.: Modeling fractional order strain in dipolar thermoelasticity. IFAC-PapersOnLine **51**(2), 601–606 (2018)
70. Yadav, A.K., et al.: Reflection of hygrothermal waves in a nonlocal theory of coupled thermo-elasticity. Mech. Adv. Mat. Struct. **31**(5), 1083–1096 (2024)

Publisher's Note